이학박사 학위논문

재현성 있는 MALDI 기술을 이용한 정량적 MALDI 이미징 및 프로파일링 조사

Investigation for quantitative MALDI Imaging and profiling with reproducible MALDI

2017년 2월

서울대학교 대학원

화학부 물리화학전공

박 경 만

A Ph. D. Thesis

Investigation for quantitative MALDI Imaging and profiling with reproducible MALDI

By Kyung Man Park

Supervisor: Seonghoon Lee

Department of Chemistry

Seoul University

February 2017

Abstract

Matrix-assisted laser desorption ionization (MALDI) combined with time-of-flight (TOF) mass spectrometry is an useful technique to analyze biomolecules. When laser irradiate on the matrix containing analytes, gas-phase ions are generated. It is well known that generating reproducible analyte ion signals is difficult and therefore it has not become the method for quantification. To overcome this problem, adding an internal standard, e.g. an isotopically labeled internal standard such as ^{13}C and ^{15}N has been implemented. Recently, MALDI spectra for some peptides under several experimental conditions were collected and were tagged with the temperature in the early MALDI plume, T_{early}. We found that the patterns of the spectra became similar, or reproducible, when those tagged with the same T_{early} were collected. To get easily reproducible MALDI mass spectra, we invented some methods to fix T_{early}. The similar MALDI mass spectra at the same T_{early} stated above meant that not only the fragmentation patterns of analyte ion, $[A + H]^+$, and matrix ion, $[M + H]^+$, but also the analyte-to-matrix ion ratio, $[A + H]^+/[M + H]^+$, was thermally determined. To check this, we implemented experiments for samples with various matrix-to-analyte

ratios, collected spectra tagged with the same T_{early}, and measured the reaction quotient $Q = ([M]/[A])([A + H]^+/[M + H]^+)$. For the matrix-to-analyte neutral ratio in the plume, [M]/[A], we used the ratio in the solid sample. Then, Q turned out to be independent of the neutral ratio, or was essentially the equilibrium constant K. The equilibrium relation can be written in the following form.

$([A + H]^+/[M + H]^+) = K ([A]/[M])$

This equation suggests that the concentration, or the amount, of an analyte in a sample can be measured from the abundances of analyte and matrix ions. We took a plot of the ion ratio versus the [A]/[M] as a calibration curve to quantify an analyte. We also defined the matrix suppression (S) as $1 – I([M + H]^+)/I_0([M + H]^+)$. $I([M + H]^+)$ and $I_0([M + H]^+)$ mean the matrix ion abundances in the spectrum of a matrix-analyte mixture and of a pure matrix, respectively. Once S exceeded a critical value, the linearity of calibration curve was broken.

Mapping the spatial distributions of interesting analytes in biological samples has attracted a lot of interest. Imaging and profiling based on mass spectrometry are particularly attractive because of its capability to determine the distribution of lots of unknown chemicals in a single measurement. Two popular ionization techniques widely used in imaging and profiling are

Secondary ion mass spectrometry (SIMS) and MALDI, especially in combination with TOF analyzer. MALDI is more useful to analyze large molecules, compared to SIMS. There are big two problems to be solved in MALDI imaging and profiling. The first is that mass spectra obtained by MALDI were irreproducible, from sample to sample, from spot to spot in a sample, and from shot to shot at a spot. Hence, there is no way to draw quantitatively meaningful image maps. The other is as in the following. The analytes are located in the sample from at first and a matrix solution is put on the sample surface and the solution dry. Finally crystals made of matrixes and analytes are formed. In this process, there is uncertainty that all analytes in the original sample are relocated in the matrix crystal, namely analyte transfer efficiency.

To verify that the first issue can be solved by our MALDI quantification method, we investigated samples with known concentrations of an analyte in the matrix crystal. For accurate results, we prepared a mixture solution consisting of both matrixes and analytes, sprayed it on a cleaned tissue, and dried the tissue. We call this premixed sample. We quantified the analytes in the premixed samples using the method invented by us and showed the quantification results were agreed with the prepared concentrations. That is, taking the analyte-to-matrix ion ratio as the measure of the analyte

concentration at a spot can be a solution to the first problem. However, the preparation method of premixed sample is far from how the MALDI imaging and/or profiling sample is prepared. In real situation, a matrix solution is put onto the sample surface and the analyte existing in the sample is extracted by the solvents. Finally the crystals containing matrixes and anayltes are formed after the solvents are dried. To check whether or not all of analytes are quantitatively extracted, we prepared a pseudo MALDI profiling sample in which the analyte and matrix solutions were loaded and dried one after another. Through the close and many studies, we found that an evaporation time of the solvents used is responsible for the analyte transfer efficiency from the sample to the matrix. We recently introduced that fluidic liquid matrixes can be made by the nonstoichiometric mixing of the organic acids and organic bases. Such a liquid is fluidic and homogeneous. More importantly, this characteristic property of the liquid matrix can be useful for the efficient extraction of analytes.

The remedy for the second problem is that choice of proper solvent which does not quickly evaporate or using the liquid matrix. In this work, the effort to unravel the problems hindering the quantitative MALDI imaging and profiling is introduced.

● Keywords: MALDI, Quantification, Imaging, Profiling, Analyte transfer,

Solvent effect, Liquid matrix

- Student Number: 2013-30902

Contents

List of Figures

List of Tables

Chapter 1

A simple method for quantification of peptides and proteins by matrix-assisted laser desorption ionization mass spectrometry

1.1 Introduction

Matrix-assisted laser desorption ionization (MALDI) and electrospray ionization are two most popular ionization techniques in mass spectrometry of biological molecules.[1-3] Sample matrix effect, or suppression of analyte ion signal,[2,4] is one of the difficulties in these techniques, especially in their use for quantitative analysis—quantification of peptides and proteins is one of the outstanding problems in quantitative proteomics.[5-9] Sample clean-up and coupling with a chromatograph are used to deal with this problem.

The fact that an analyte ion signal can be observed even when contaminants are present in a sample and that spectral acquisition can be

made rapidly are distinct advantages of MALDI mass spectrometry.[10-12] However, MALDI is not regarded as the method of choice for quantitation because analyte ion signals generated by this technique display poor sample-to-sample, spot-to-spot, and shot-to-shot reproducibilities.[13] The best way to cope with the signal irreproducibility has been to add an internal standard whose physicochemical properties are similar to those of the analyte. The analyte molecules that are chemically or metabolically labeled with stable isotopes such as ^{13}C and ^{15}N can be useful for this purpose.[14-19] One of the problems in this approach is that the complexity of biological samples sometimes makes it difficult to find an internal standard with an m/z different from all the substances in the sample. Another problem is that you need an isotopically labeled internal standard for each analyte to be quantified. The latter problem can be avoided by tagging the analyte with an isotopically labeled reagent.[20-22] For example, in the method called ICAT (isotope-coded affinity tag)[20] developed for the quantification of proteins, a part of the tag called linker is labeled with stable isotopes. Sample loss and long analysis time are the potential problems common to the analytical schemes utilizing on-site chemical labeling.

Recently, we investigated MALDI of some peptides by collecting mass

spectra from different samples, from different spots on the same sample, and from different laser shots on the same spot.[23] We estimated the effective temperature in the early matrix plume, T_{early}, associated with each spectrum by kinetic analysis of the fraction of peptide ions that did not dissociate until they passed the ion source exit, or the survival probability.[24] Then, we observed that the overall patterns of MALDI spectra obtained under different experimental conditions were similar, or reproducible, when those associated with the same T_{early} were compared. In particular, the reaction quotient for the matrix-to-peptide proton transfer was constant regardless of the peptide concentration in the solid sample.[23] Kinsel et al.[25] observed near equilibrium in MALDI of amino acids even without temperature selection. There, the observed near equilibrium arose possibly because only the spectral data collected in a narrow range of shots were compared and hence the temperature did not change much. From the near constancy of the reaction quotient for the matrix-to-peptide proton transfer at a specified temperature, we realized that this would allow us to quantify analytes by MALDI without adding any internal standard. Such a capability will be demonstrated in this work for some peptides and proteins.

1.2 Experimental

Two homebuilt MALDI-TOF instruments were used, instruments I[26] and II.[27] Overall layouts for the two instruments are similar, even though they differ in details such as in the total length. In each instrument, 337 nm output from a nitrogen laser (MNL100, Lasertechnik Berlin, Berlin, Germany) was used for MALDI. The focal lengths of the lenses were 100 and 250 mm, respectively, for the instruments I and II. Instrument I was used mostly for MALDI with α-cyano-4-hydroxycinnamic acid (CHCA) as the matrix, while instrument II was for MALDI with 2,5-dihroxybenzoic acid (DHB). The threshold laser pulse energies were 0.30 and 1.65 μJ/pulse, respectively, for CHCA- and DHB-MALDI. Spectral measurements were made using the laser pulse energy corresponding to two times the threshold.[28] Quantification results for the same peptides were the same within error limits regardless of the instrument used. To improve the signal-to-noise ratio, spectral data from every ten laser shots were summed. Then, the results from twenty different spots on a sample were summed. Detector gain vs. m/z of ion was calculated by measuring the charge for each single ion pulse. The number of ions in each peak was calculated by integrating its current vs. TOF data and dividing the result by the detector gain.[29,30]

Sample preparation: Angiotensin I (DRVYIHPFHL), angiotensin II (DRVYIHPF), substance P (RPKPQQFFGLM-NH_2), YGGFL, insulin, β-amyloid 1-42, CHCA, and DHB were purchased from Sigma (St. Louis, MO, USA). Remaining peptides were purchased from Peptron (Daejeon, Korea). Non-peptide samples, i.e. histamine, glucosamine, fumonisin B1, and creatinine were also purchased from Sigma.

Aqueous stock solution of each analyte except insulin was diluted to a desired concentration and mixed with 1:1 water/acetonitrile solution of CHCA or DHB. In the case of insulin, acetonitrile was used to prepare stock solution. 1 μL of a mixture was loaded on the target and vacuum-dried. With CHCA, spectral data were taken from any location on a solid sample because samples prepared by vacuum-drying were rather homogeneous. In the case of DHB, crystallites at the rim of a sample were much larger than those near the center. For ease of experiment, spectral data were taken from the center.

1.3 Results and Discussion

Since a sample used in MALDI is a mixture of a matrix (M) and an analyte (A), the overall pattern of a MALDI spectrum would be determined by three factors. First are the fragment ion-to-precursor ion (AH^+) abundance ratios for the analyte. Second are the fragment ion-to-precursor ion (MH^+) abundance ratios for the matrix. Third is the analyte ion-to-matrix ion abundance ratio, $[AH^+]/[MH^+]$.[23] Then, the similar overall pattern at the same T_{early} mentioned in a previous section meant that not only the relative abundances of the fragment ions from AH^+ and MH^+ but also the $[AH^+]/[MH^+]$ ratio was thermally determined. This, in turn, suggested that the reaction quotient for the matrix-to-peptide proton transfer, $MH^+ + A \rightarrow M + AH^+$, was nearly constant at the temperature of T_{early}.[23] To check this, we performed experiments for samples with various matrix-to-analyte ratios, selected spectra associated with the same T_{early}, and estimated the reaction quotient $Q = ([M]/[A])([AH^+]/[MH^+])$.[23] Assuming that the proton transfer preceded the fragmentation of AH^+ and MH^+, we estimated $[AH^+]$ and $[MH^+]$ as the sums of the analyte- and matrix-derived ions, respectively. However, as far as checking the constancy of Q was concerned, the abundance of any analyte-derived ion, whether it was AH^+, one of its fragments, or their

combinations, might as well be used because the abundance of each fragment ion relative to that of AH^+ was fixed when T_{early} was specified. The same applied to $[MH^+]$. For the matrix-to-analyte neutral ratio in the plume, [M]/[A], we used the ratio in the solid sample. Then, Q turned out to be independent of the matrix-to-analyte ratio. Even though the constancy of Q is generally taken as manifestation of equilibrium, a kinetic quasi-steady state may be a better description for the situation in the early matrix plume because it is undergoing a rapid time evolution.[31] The above relation can be written in the following form.

$$[AH^+]/[MH^+] = Q\,([A]/[M]) \qquad (1.1)$$

With Q constant, the analyte-to-matrix ion abundance ratio measured from a spectrum is directly proportional to the analyte-to-matrix ratio in the solid sample. Such a direct proportionality holds only when the ion abundance data are taken from the spectra associated with the same T_{early}. Eq. (1.1) suggests that the concentration, or the amount, of an analyte in a solid sample can be determined from the abundances of analyte- and matrix-derived ions. From the description of the method used to calculate Q, it is obvious that the abundance of any ion derived from the analyte, and from the matrix also, can be used for the analysis. In the case of the analyte, its

molecular ion (AH^+) would be the natural choice.

When there are two analytes, A and A′, in a sample, a relation similar to eq. (1.1) will hold for the second component also.

$$[A'H^+]/[MH^+] = Q' ([A']/[M]) \qquad (1.2)$$

Regardless of the participation of the second proton transfer reaction, however, eq. (1.1) may hold. That is, analyte quantification based on eq. (1.1) may be made even when the analyte is a component of a mixture. Another important aspect of the present quantification scheme is that one does not have to add an internal standard. Or, one may say that the matrix is serving as the internal standard.

Spectral selection: It is well known that some of the matrix and peptide ions undergo dissociation in the hot early matrix plume—in-source decay (ISD).[24,32] Intuitively, ISD will become more efficient as the early plume gets hotter. In a previous study, we treated the internal energy of a peptide ion undergoing ISD as displaying thermal distribution at an effective temperature, T_{early}. Then, we devised a method to determine T_{early} by kinetic analysis of the probability for a peptide ion to avoid ISD until it passed the source exit, that could be calculated from a MALDI spectrum.[24,28] The method requires knowledge on the rate-energy relation, k(E), for the dissociation of this ion

that must be determined by a separate study. An easier way to estimate T_{early} is to utilize the fact that the extent of fragmentation for a matrix ion is thermally determined also.[23] In this work, we took CHCA-MALDI spectra of Y_5K—dissociation kinetics of $[Y_5K + H]^+$ was determined previously[33]—and calculated T_{early} associated with each spectra. From the abundance vs. T_{early} data for several matrix-derived ions, we decided to use the $[M + H - H_2O]^+$-to-$[M + H]^+$ ion abundance ratio as a measure of T_{early}. This ion abundance ratio vs. T_{early} data are shown in Figure 1.1(a). For example, this ratio of 3.0-4.5 corresponds to T_{early} of 870-900 K. We did the same for DHB-MALDI utilizing the dissociation kinetics of $[Y_6 + H]^+$ (Figure 1.1(b)).[33] In this case, the $[M + H - H_2O]^+$-to-$[M + H]^+$ ratio of 4.0-11.5 in DHB-MALDI corresponds to T_{early} of 780-800 K. We would like to emphasize that the accuracy of the present method is not critical and that the magnitude of the number evaluated is meaningless because we use it only to select spectra associated with the same T_{early}.

In the previous study on the reproducibility of temperature-selected MALDI spectra,[23] we did not deal with DHB-MALDI because the spot-to-spot spectral variation was more serious than in CHCA-MALDI. In this work, we collected spectral data from the central part, rather than the rim, of a dried

DHB sample to reduce such variation.

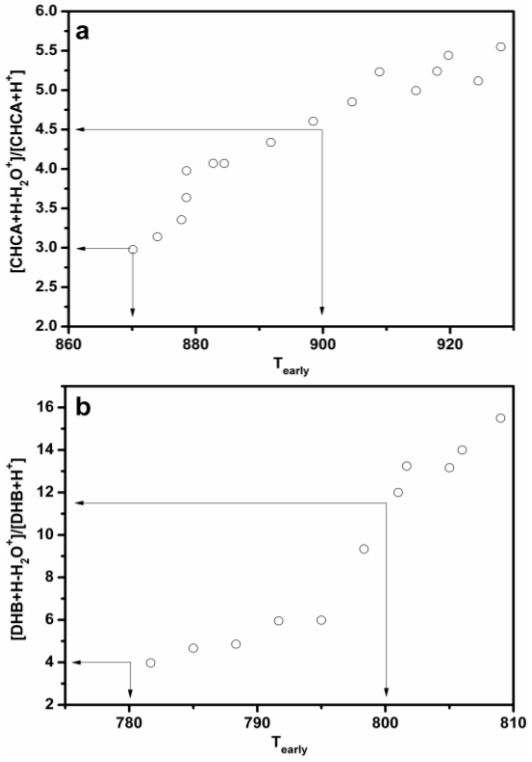

Figure 1.1 $[M + H - H_2O]^+$-to-$[M + H]^+$ ion abundance ratio vs. T_{early} for (a) CHCA and (b) DHB. T_{early} was determined by kinetic analysis of the survival probability of a peptide ion at the ion source exit. To calculate T_{early}, Y_5K and Y_6 were used in CHCA- and DHB-MALDI, respectively. For CHCA-MALDI, the $[CHCA + H - H_2O]^+$-to-$[CHCA + H]^+$ ratio of 3.0-4.5 corresponds to the T_{early} range of 870-900 K. For DHB-MALDI, the $[DHB + H - H_2O]^+$-to-$[DHB + H]^+$ ratio of 4.0-11.5 corresponds to the T_{early} range of 780-800 K.

Table 1.1 Quantification results[a]

Matrix	CHCA (Figure 1.4)[b]			CHCA (Figure 1.5)[b]			DHB (Figure 1.6)[c]		
Analyte	Amount loaded	Amount determined		Amount loaded	Amount determined		Amount loaded	Amount determined	
		Calibration curve	One-point calibration		Calibration curve	One-point calibration		Calibration curve	One-point calibration
YLYEIAR	0.30	0.29±0.05	0.30±0.04	0.10	0.13±0.02	0.13±0.02	0.30		0.30±0.04
Y_5K	0.30	0.23±0.03	0.21±0.03	1.0	0.78±0.08	0.79±0.08	0.30	0.24±0.02	0.22±0.02
DLGEEHFK	0.30		0.20±0.03	3.0		2.1±0.4	0.30		0.23±0.01
Y_5R	0.30	0.24±0.03	0.25±0.04	0.30	0.34±0.04	0.37±0.05	0.30	0.22±0.04	0.24±0.05
DRVYIHPF	0.30	0.29±0.02	0.24±0.02				0.30		0.21±0.04
FKDLGEEHFK	0.30		0.36±0.04				0.30		0.35±0.08
DRVYIHPFHL	0.30		0.38±0.11						
HLVDEPQNLIK	0.30		0.36±0.03				0.30		0.34±0.07
RPKPQQFFGLM-NH_2	0.30		0.31±0.01				0.30		0.29±0.10
YGGFL				10		11±3			
Histamine				1.0		0.74±0.15			
Glucosamine				30		24±5			
Fumonisin B1				1.0		0.89±0.29			
Creatinine				0.30		0.21±0.02			
β-amyloid 1-42							3.0		3.2±0.7
Insulin							3.0	3.3±0.7	2.7±0.6

[a]Errors denote one standard deviations from triplicate measurements.

[b]Amount in number of picomoles of an analyte in 25 nmol of CHCA.

[c]Amount in number of picomoles of an analyte in 50 nmol of DHB.

Calibration curve: To check the utility of eq. (1.1) in analyte quantification, we carried out MALDI studies for solid samples with 0.01-250 pmol Y_5R, Y_5K, YLYEIAR, or angiotensin II in 25 nmol CHCA. For each sample, we obtained a set of spectra as a function of the laser shot number, selected those with the $[CHCA + H - H_2O]^+$-to-$[CHCA + H]^+$ ion abundance ratio lying in the range of 3.0-4.5 (870-900 K in T_{early}), and calculated $[AH^+]/[MH^+]$ for the selected spectra. We took the abundance of protonated peptides as $[AH^+]$ while the sum of the abundances for $[CHCA + H]^+$, $[CHCA + H - H_2O]^+$, and $[CHCA + H - CO_2]^+$ was taken as $[MH^+]$. The log-log plots of $[AH^+]/[MH^+]$ vs. [A]/[M] obtained for the four peptides are shown in Figure 1.2. In the four plots, it is obvious that $[AH^+]/[MH^+]$ is directly proportional to [A]/[M] up to around 30 pmol of a peptide in 25 nmol of CHCA—the reason for the deviation from linearity at higher peptide concentration is under investigation. We also observed direct proportionality for the calibration curves for DHB-MALDI of Y_5R, Y_5K, and insulin in Figure 1.3. Direct proportionality in the calibration curve suggests that an analyte can be quantified rapidly by one-point calibration, i.e. by utilizing the ion abundance data at one concentration. In practice, we utilized the data obtained at 3-10 times the concentration of the analyte to be quantified.

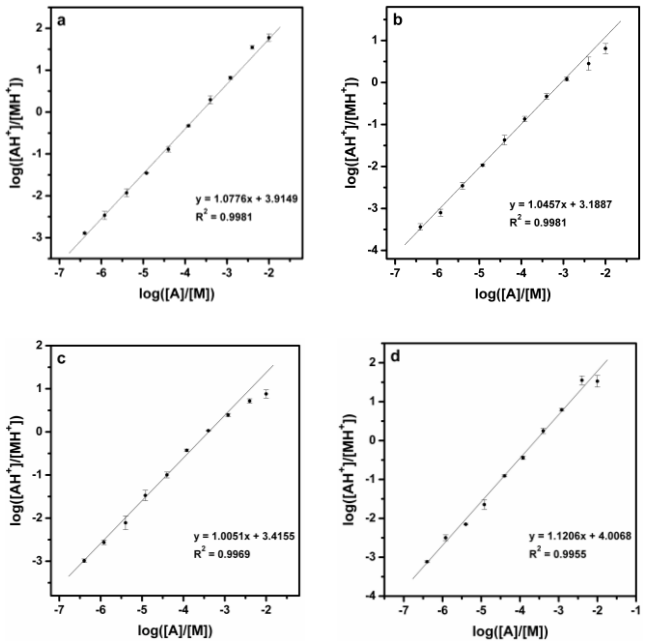

Figure 1.2 Calibration curves in CHCA-MALDI of (a) Y_5R, (b) Y_5K, (c) YLYEIAR, and (d) angiotensin II. $[AH^+]/[MH^+]$ vs. [A]/[M] is drawn in log-log scale. The amount of each peptide, 0.01-250 pmol, in 25 nmol of CHCA in a solid sample was used to calculate [A]/[M]. $[AH^+]/[MH^+]$ was calculated from MALDI spectra with the $[CHCA + H - H_2O]^+$-to-$[CHCA + H]^+$ ion abundance ratio of 3.0-4.5 (870-900 K in T_{early}). The abundance of the protonated peptide was taken as $[AH^+]$ while the sum of the abundances of $[CHCA + H]^+$, $[CHCA + H - H_2O]^+$, and $[CHCA + H - CO_2]^+$ was taken as $[MH^+]$. Error bars indicate one standard deviation from triplicate measurements.

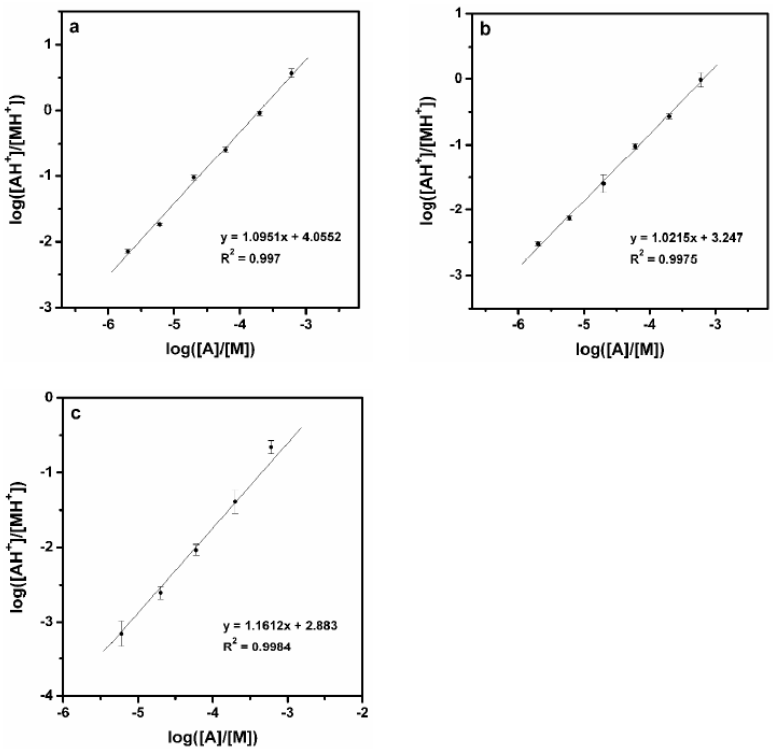

Figure 1.3 Calibration curves for DHB-MALDI of (a) Y_5R, (b) Y_5K and (c) insulin drawn in log-log scale. A solid sample consisted of 50 nmol DHB and 0.1-30 pmol of Y_5R or Y_5K, or 0.3-30 pmol of insulin. Two times the threshold laser pulse energy was used. MALDI spectra with the $[DHB + H - H_2O]^+$-to-$[DHB + H]^+$ ion abundance ratio of 4.0-11.5 (780-800 K in T_{early}) were selected. The abundance of the protonated peptide was taken as $[AH^+]$ while the sum of the abundances of $[DHB + H]^+$ and $[DHB + H - H_2O]^+$ were taken as $[MH^+]$. Error bars indicate one standard deviation from triplicate measurements.

MALDI of mixtures: Even when the calibration curve for a pure analyte displays good direct proportionality, quantification of the same analyte present as a component of a mixture can be difficult due to the suppression effect by others. To test such a possibility, we prepared an equimolar mixture of nine peptides (YLYEIAR, Y_5K, DLGEEHFK, Y_5R, DRVYIHPF, FKDLGEEHFK, DRVYIHPFHL, HLVDEPQNLIK, and RPKPQQFFGLM-NH_2), 0.3 pmol each in 25 nmol CHCA, and took its MALDI spectra. From these we obtained a spectrum by summing those with the $[CHCA + H - H_2O]^+$-to-$[CHCA + H]^+$ ratio of 3.0-4.5 (870-900 K). We also obtained one-analyte MALDI spectra for each peptide, 0.3 pmol in 25 nmol CHCA. In Figure 1.4, four temperature-selected single-peptide MALDI spectra are compared with the nine-peptide MALDI spectrum. All the spectra in the figure are normalized to the abundance of $[CHCA + H - H_2O]^+$. It is obvious from the figure that the relative abundance of a peptide ion is similar whether the peptide is the only analyte in the sample or is a component of the mixture. According to eq. (1.1), the relative abundance of a peptide ion, represented by $[AH^+]/[MH^+]$ for convenience, is proportional to the peptide concentration in the solid sample, [A]/[M]. When [A]/[M] iskept the same, $[AH^+]/[MH^+]$ is the same regardless of the presence of other analytes in the

sample. Presence of other analytes reduces the abundance of a selected analyte ion indirectly, by reducing [MH^+]. An analyte ion may appear weakly in the MALDI spectrum of a mixture either because its concentration ([A]/[M]) is low or because it is a weak base.

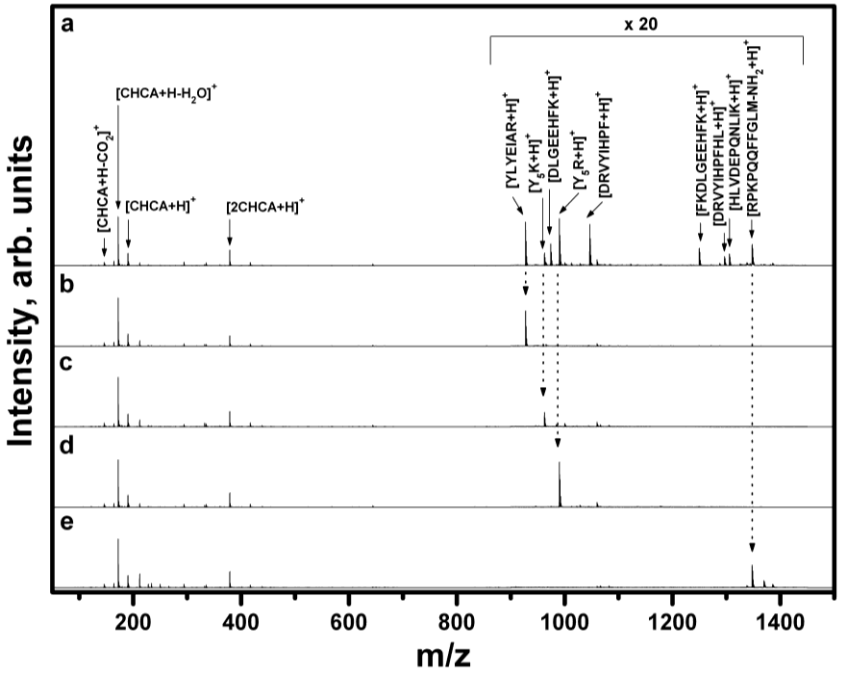

Figure 1.4 (a) MALDI spectrum for an equimolar mixture of nine peptides (YLYEIAR, Y_5K, DLGEEHFK, Y_5R, DRVYIHPF, FKDLGEEHFK, DRVYIHPFHL, HLVDEPQNLIK, and RPKPQQFFGLM-NH_2), 0.30 pmol each in 25 nmol CHCA. (b)-(e) are MALDI spectra of 0.30 pmol of one peptide in 25 nmol of CHCA for (b) YLYEIAR, (c) Y_5K, (d) Y_5R, and (e) RPKPQQFFGLM-NH_2. Temperature selection was made by selecting spectra with $[CHCA + H - H_2O]^+$-to-$[CHCA + H]^+$ ratio of 3.0-4.5 (870-900 K). Each spectrum was normalized to the abundance of $[CHCA + H - H_2O]^+$.

Quantification: Y_5K, Y_5R, YLYEIAR, and angiotensin II in the above peptide mixture were quantified by using the calibration curve for each. All the peptides were also quantified by one-point calibration using the data obtained from a single-analyte sample containing 1.0 pmol of each peptide in 25 nmol CHCA. The results obtained by triplicate measurements are listed in Table 1.1. It is to be noted that one-point calibration produced as good results as produced by calibration curves. In biological samples of peptide mixtures, the amount of each peptide may be widely different and materials other than peptides may be present. To mimic the situation, a mixture containing nine analytes with various amounts, i.e. YLYEIAR (0.10), Y_5K (1.0), DLGEEHFK (3.0), Y_5R (0.30), YGGFL (10), histamine (1.0), glucosamine (30), fumonisin B1 (1.0), and creatinine (0.30), were prepared. Here the number in each parenthesis denotes the number of picomole of each analyte in 25 nmol of CHCA. The CHCA-MALDI spectrum of the sample is shown in Figure 1.5 and the quantification results are listed in Table 1.1. Even though YLYEIAR, Y_5K, and DLGEEHFK were present in the samples used for Figures 1.4 and 1.5, their concentrations were different. In each case, the quantification result was close to the actual amount in the sample. We also attempted quantification using DHB as the matrix. Temperature-selected

(780-800 K) MALDI spectrum obtained from a mixture containing 3.0 pmol of β-amyloid 1-42, 3.0 pmol of insulin, and 0.30 pmol each of YLYEIAR, Y_5K, DLGEEHFK, Y_5R, DRVYIHPF, FKDLGEEHFK, HLVDEPQNLIK, and RPKPQQFFGLM-NH_2 in 50 nmol of DHB is shown in Figure 1.6. We attempted quantification of Y_5R, Y_5K, and insulin using calibration curves shown in Figure 1.3. All the analytes were also quantified by one-point calibration using the single-analyte data at ten times the concentration in each case. The results are also listed in Table 1.1. In all the cases, the quantification error estimated as one standard deviation in triplicate measurements was around ±30%.

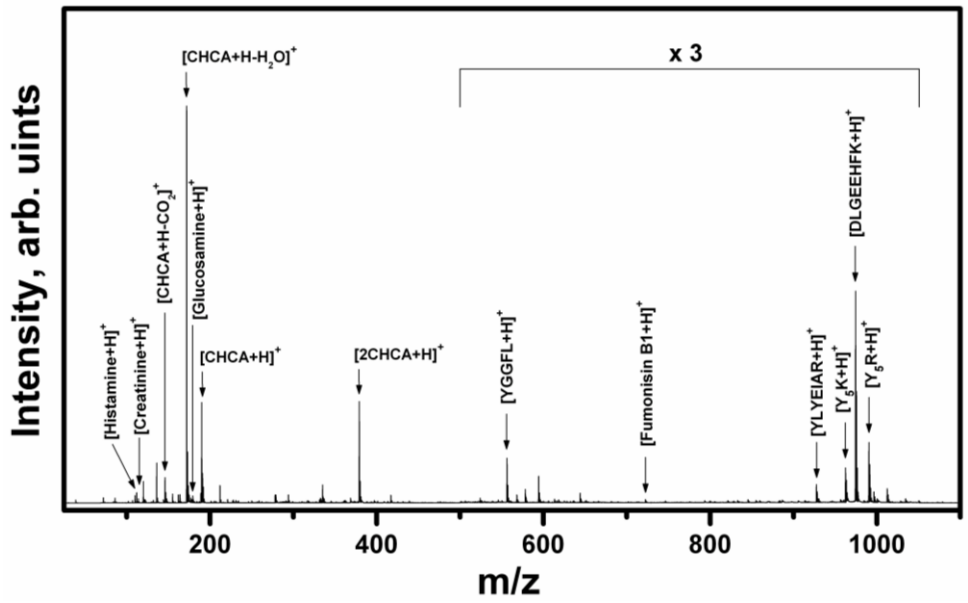

Figure 1.5 MALDI spectrum for a mixture of nine analytes, i.e. YLYEIAR (0.10), Y_5K (1.0), DLGEEHFK (3.0), Y_5R (0.30), YGGFL (10), histamine (1.0), glucosamine (30), fumonisin B1 (1.0), and creatinine (0.30). Here the number in each parenthesis denotes the number of picomole of each analyte in 25 nmol of CHCA. Temperature selection was made by selecting spectra with $[CHCA + H - H_2O]^+$-to-$[CHCA + H]^+$ ratio of 3.0-4.5 (870-900 K).

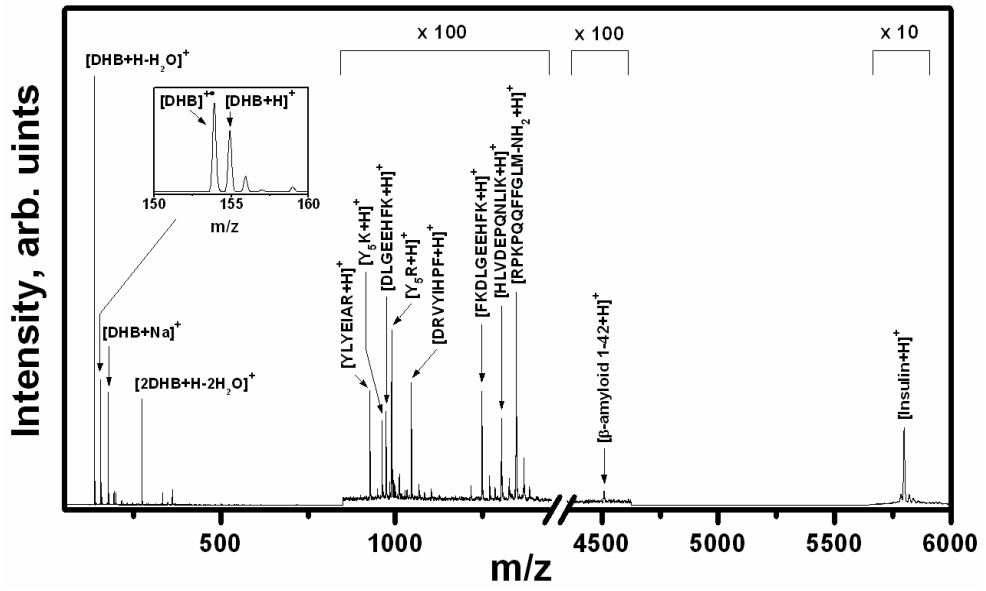

Figure 1.6 MALDI spectrum for a mixture containing 3.0 pmol of β-amyloid 1-42, 3.0 pmol of insulin, and 0.3 pmol each of YLYEIAR, Y_5K, DLGEEHFK, Y_5R, DRVYIHPF, FKDLGEEHFK, HLVDEPQNLIK, and RPKPQQFFGLM-NH_2 in 50 nmol of DHB. Temperature selection was made by collecting spectra with the $[DHB + H - H_2O]^+$-to-$[DHB + H]^+$ ratio of 4.0-11.5 (780-800 K in T_{early}).

1.4 Conclusion

Even though MALDI is a sensitive, rapid, and relatively inexpensive method for the analysis of biological molecules, its utility in their quantification has been limited due to the poor spectral reproducibility. In this work, our previous observation that temperature-selected MALDI spectra were reproducible has been translated into the direct proportionality between the analyte-to-matrix ion abundance ratio and the analyte-to-matrix ratio in the solid sample, allowing easy quantification of the analyte. The relation has been found to hold even when the analyte is a component of a mixture. A salient feature of the method is that one can quantify an analyte without adding an internal standard. In this sense, the present method might be classified as a highly systematic version of an external standard method. Alternatively, it might be classified as an absolute quantification method using matrix as the internal standard. We expect that the method will become an inexpensive technique suitable for quick quantitative screening of any analyte amenable to MALDI such as peptides and proteins. The fact that the analyte concentration is proportional to the analyte-to-matrix ion abundance ratio can be used for very quick comparison of the relative amounts of a particular analyte in two or more biological samples.

Chapter 2

Relative quantification in imaging of a peptide on a mouse brain tissue by matrix-assisted laser desorption ionization

2.1 Introduction

Determining the spatial distributions of biological or pharmaceutical molecules in tissue samples is of current interest.[34-39] Imaging methods based on mass spectrometry (mass spectrometric imaging, MSI)[36-39] are particularly attractive because of its capability to identify analyte molecules. Here, mass spectra generated by a technique for gas-phase ion formation from samples in condensed phases are acquired at many locations on a tissue. Then, the abundances of an ion with a particular mass-to-charge ratio are plotted in the form of a two-dimensional image map. Secondary ion mass spectrometry (SIMS)[40,41] and matrix-assisted laser desorption ionization

(MALDI) are two popular ion formation techniques that are widely used in MSI, especially in combination with time-of-flight (TOF) mass analysis. Compared to SIMS, MALDI is more useful for generating molecular ions of large labile biological molecules.[38] On the other hand, the spatial resolution in MALDI is poorer than in SIMS. Progresses are being made to lessen the weaknesses of each technique.

In the interpretation of MALDI imaging data, it is implicitly presumed[42] that the abundance of an ion measured at a particular location increases with the amount of the corresponding analyte molecule at the same two-dimensional location in the original tissue. This assumption consists of two preconditions. First is that the amount of the analyte available for ionization at a particular two-dimensional location is a good representation of its amount at the same location inside the original tissue. Second is that the measured ion abundance increases with the amount of the analyte. It is to be noted that if the rule governing the relation between the amount of an analyte and the measured ion abundance—this pertains to the second assumption—is unknown, even the validity of the first assumption cannot be checked. Recently, it was reported that the chemical environment of an analyte also affected the measured ion abundance, which is often called ‘ion

suppression'.[43,44] With severe ion suppression in MALDI at a spot, an ion signal might be difficult to observe even when a large amount of the corresponding analyte is present at the spot, a case against the utility of MSI.

For many years, it was widely thought that ion signals generated by MALDI were irreproducible, from sample to sample, from spot to spot in a sample, and from shot to shot at a spot.[13,45] Hence, development of the current MALDI-based MSI[46] that can generate reproducible images in favorable cases should be regarded as a real achievement, although there is no guideline to check the quantitative validity of such images.

Recently,[23] we found that the overall pattern of and the abundance of each ion appearing in the MALDI-TOF spectrum of a peptide became reproducible when the effective temperature, T_{early}[28], in the early plume where the in-source decay[47] occurred was kept constant. We also found[48] that the matrix-to-peptide proton transfer occurring in the plume was in quasi-equilibrium and resulted in the following relation.

$$I([P + H]^+)/I([M + H]^+) = K\, I(P)/I(M) \qquad (2.1)$$

Here, I represents the abundance of a matrix (M)- or peptide (P)-derived species in the plume and K is the equilibrium constant. $I(P)/I(M)$ in the plume was taken to be the same as the corresponding ratio, or peptide

concentration, in the solid sample. Direct proportionality between $I([P+H]^+)/I([M+H]^+)$ and $I(P)/I(M)$ in eqn. (2.1) is essentially a calibration relation that can be used for the quantification of the peptide.[48] It is to be emphasized that the peptide concentration in the solid sample is proportional to $I([P+H]^+)/I([M+H]^+)$, not to the peptide ion abundance, $I([P+H]^+)$, itself. Also to be emphasized is that eqn. (2.1), which is an equilibrium relation, will hold even when other reactions also occur in the plume and are in quasi-equilibrium. We found[49] that the linear relation in eqn. (2.1) held as long as the matrix suppression, S, was small, e.g. 70% or less when α-cyano-4-hydroxycinnamic acid (CHCA) was the matrix.

$$S = 1 - I([M+H]^+)/I_0([M+H]^+) \qquad (2.2)$$

Here, $I_0([M+H]^+)$ is the matrix ion abundance in MALDI of the pure matrix.

Our quantification method for peptides by MALDI is based on two pillars, i.e. acquisition of spectra at a constant T_{early} and their analysis with eqn. (2.1). The method was tested for various samples of matrix-peptide mixtures loaded on stainless steel targets.[48,49] In this work, we will show that the method also works for the relative quantification of peptides in samples loaded on mouse brain tissues.

2.2 EXPERIMENTAL SECTION

All the measurements were made with a home-built MALDI-tandem TOF apparatus described previously[53]. The apparatus consists of an ion source with delayed extraction, an ion gate, a reflectron, and a microchannel plate detector just as for most conventional instruments. The accelerating voltage in the source is 21.5 kV. 337 nm output from a nitrogen laser (MNL100, Lasertechnik Berlin, Berlin, Germany) is focused on the sample to an ellipse with the semimajor (y) and semiminor (z) axes of ~65 and ~25 μm, respectively. The area of a peak in a mass spectrum was taken as the relative abundance of the corresponding ion. This was converted to the number of ions by taking into account the detector gain.[50] Operation of the instrument including temperature control and data acquisition and processing were carried out by home-made software.

As mentioned earlier, MALDI spectra of a sample become reproducible when the temperature in the early plume, T_{early}, is kept constant. As measures of T_{early}, we initially utilized the extent of fragmentation of a peptide ion or a matrix ion.[28,48] Later,[51] we observed that the total number of particles hitting the detector (loosely called total ion count, or TIC) was a good measure of T_{early}. The method to keep T_{early} constant is as follows.[51] For a fresh sample,

we measure the threshold pulse energy for MALDI. This is ~0.4 μJ per pulse when CHCA is the matrix. Typically, we begin spectral acquisition using two times the threshold pulse energy. TIC measured for a fresh sample at this pulse energy is ~1500 counts per pulse, which is taken as the preset value. As the irradiation at a spot continues, T_{early} goes down and hence TIC decreases. Then, we raise the pulse energy to bring TIC back to the preset value. Eventually, depleted regions begin to appear on the irradiated spot, typically when the pulse energy increases to three times the threshold.

In a typical imaging experiment, 50 and 10 spots along the y and z axes, respectively, were chosen at the interval of 150 μm. From the data collected at many spots, an image map was constructed using a commercial software (Origin, version 8.0, Northampton, MA, USA).

Reagents and sample preparation. Peptides Y_5R and YLYEIAR were purchased from Peptron (Daejeon, Korea). All the other chemicals were purchased from Sigma (St. Louis, MO, USA).

5 μm thick mouse brain tissues[52] were prepared following the method in ref. 53. Two different procedures, Procedure I and II, were used to clean the tissues. In Procedure I, a tissue was dipped twice in 7:3 ethanol/water for 30 seconds. In Procedure II, a tissue treated by Procedure I was further dipped

twice in 100% ethanol for 30 seconds. Naturally, the tissues prepared by Procedure II were cleaner.

Sample solutions containing CHCA and peptides were prepared with 1:1 acetonitrile/water. A commercial device (ImagePrep, Bruker Daltonik GmbH, Bremen, Germany) was used to spray-coat a tissue with a sample solution. The protocol recommended by the manufacturer for spraying CHCA solution was used.

2.3 RESULTS AND DISCUSSION

Principle of the method. The strategy we adopted to estimate the relative amount of a peptide at a spot from ion signals in MALDI is as follows.

1. Implicitly, it is thought that a fairly even thickness of matrix layer throughout a tissue is a requirement for reliable imaging. As mentioned in the previous section, we estimated the thicknesses of the matrix layer at each spot and used it as a measure of sample quality.

2. TIC is kept constant throughout the measurement for a tissue sample. As shown in an earlier report,[54] K and the amount of materials ablated per laser shot that is essentially I(M) in eqn. (2.1) are constant when TIC is kept constant. Then, when the thickness of the matrix layer is similar throughout the sample, the number of single-shot spectra that can be acquired from each spot would be similar.

3. With I(M) and K kept constant, eqn. (2.1) for the *i*th shot at a spot becomes as follows.

$$\mathrm{I}_i([\mathrm{P}+\mathrm{H}]^+)/\mathrm{I}_i([\mathrm{M}+\mathrm{H}]^+) = \mathrm{K}\,\mathrm{I}_i(\mathrm{P})/\mathrm{I}(\mathrm{M}) \qquad (2.3)$$

Summing over the total number of shots at a spot and rearranging, eqn. (2.3) is converted as follows.

$$\mathrm{I}_{total}(\mathrm{P}) = \{\mathrm{I}(\mathrm{M})/\mathrm{K}\}\sum_i\{\mathrm{I}_i([\mathrm{P}+\mathrm{H}]^+)/\mathrm{I}_i([\mathrm{M}+\mathrm{H}]^+)\} \qquad (2.4)$$

Here, $I_{total}(P)$ represents the total amount of the peptide at the spot where the measurement has been made. Eqn. (2.4) tells us that this is proportional to $\sum_i\{I_i([P+H]^+)/I_i([M+H]^+)\}$ measured at the spot, not to $\sum_i I_i([P+H]^+)$. $\sum_i I_i([P+H]^+)$ does not increase as rapidly as the peptide concentration because the amount of the matrix ion in the plume is reduced due to the matrix-to-peptide proton transfer. That is, 'ion suppression' occurs by way of 'matrix suppression'.

4. An analyte ion signal may also be suppressed due to salts and basic contaminants.[38,55] Previously,[49] we showed that we could handle the matrix suppression by basic contaminants by using eqn. (2.1) and by keeping the matrix suppression low, e.g. 70% or less when CHCA was the matrix. So far, we have not reported any result concerning the influence of the contamination by salts on the quantification of peptides. The fact that the matrix suppression by salts can also be handled by eqn. (2.1) is shown in Table 2.1.

Relative quantification of a peptide loaded on a mouse brain tissue. Earlier, we pointed out that a quantitative imaging by MALDI was hampered by two problems, one concerned with the analyte transfer from tissue to matrix layer and the other with MALDI of the analyte in the matrix layer. In

this paper, we would like to demonstrate that the method we developed for peptide quantification by MALDI, i.e. maintaining TIC constant, keeping the suppression low, and using eqn. (2.1), can solve the second problem. To avoid complications that might be caused by the first problem, we decided to analyze a peptide that had been spray-coated on a tissue together with a matrix rather than those that had originated from the tissue.

We first prepared tissues displaying very small matrix suppression by cleaning them according to Procedure II described in the experimental section. We spray-coated a cleaned tissue with CHCA, acquired its MALDI spectrum, and compared it with a similar spectrum acquired from an uncleaned tissue (not shown). The abundance of $[CHCA + Na]^+$ at m/z 212 and that of a lipid-derived ion at m/z 184 were very small in the former spectrum compared to those in the latter spectrum. Instead, the matrix-derived ions of $[CHCA + H]^+$, $[CHCA + H - H_2O]^+$, $[CHCA + H - CO_2]^+$, and $[2CHCA + H]^+$ got prominent, indicating very small suppression. Using tissues cleaned by Procedure II, we prepared two samples, tissues A and B, by spray-coating them with 1:1 acetonitrile/water containing 25 nmol of CHCA per μL and Y_5R. The concentrations of Y_5R in solutions used to prepare tissues A and B were 1.5 and 15 pmol μL^{-1}, respectively. MALDI

spectra acquired from tissues A and B are shown in Figures 2.1(a) and 2.1(b), respectively. We evaluated $\sum_i \mathrm{I}_i([\mathrm{P}+\mathrm{H}]^+)$ and $\sum_i\{\mathrm{I}_i([\mathrm{P}+\mathrm{H}]^+)/\mathrm{I}_i([\mathrm{M}+\mathrm{H}]^+)\}$ and took their averages for each tissue. The results are shown in Table 2.2.

Table 2.1 Influence of the NaCl concentration in solid samples on various quantities.

Amount of NaCl[a] (pmol)	**I([P + H]$^+$)**	**I([P + H]$^+$) /I([M + H]$^+$)**	**S, %**
0	680 ± 60	0.22 ± 0.02	26 ± 1
25	620 ± 40	0.24 ± 0.03	36 ± 4
250	490 ± 60	0.22 ± 0.04	46 ± 4
1250	370 ± 60	0.20 ± 0.01	52 ± 8

[a] In 25 nmol of CHCA containing 5.0 pmol of Y_5R

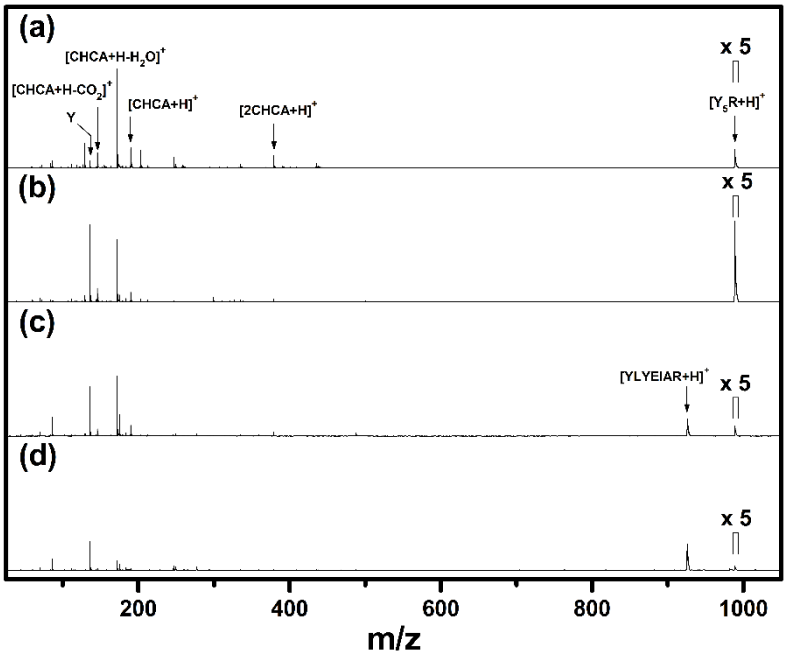

Figure 2.1 MALDI spectra of Y_5R acquired from tissues prepared in various ways. We cleaned each tissue by Procedure II. Spectra 1(a) and 1(b) were acquired from tissues that were spray-coated with a solution containing 25 nmol of CHCA per μL and 1.5 and 15 pmol per μL of Y_5R, respectively. Both spectra 1(c) and 1(d) were acquired from regions contaminated by YLYEIAR. To acquire spectra 1(c) and 1(d), 4 μL of a solution containing 200 and 600 pmol of YLYEIAR, respectively, was loaded at one location on the tissue. After the solvent evaporation, the tissue was spray-coated with a solution containing 25 nmol of CHCA and 1.5 pmol of Y_5R per μL.

Table 2.2 Analyte (Y_5R) signals from mouse brain tissues spray-coated with a solution containing 25 nmol μL^{-1} of CHCA, Y_5R, and a peptide contaminant.

Tissue	**Y_5R concentration (pmol μL^{-1})**	**contaminant**	$\sum_i \mathbf{I}_i([\mathbf{P}+\mathbf{H}]^+)^a$	$\sum_i \{\mathbf{I}_i([\mathbf{P}+\mathbf{H}]^+)/\mathbf{I}_i([\mathbf{M}+\mathbf{H}]^+)\}$
A	1.5		4000 ± 1200	1.4 ± 0.4
B	15		17000 ± 5000	14 ± 4.1
C[b]	1.5	YLYEIAR	1400 ± 500	1.6 ± 0.5

[a]In arbitrary unit.

[b]Data evaluated from the spectra acquired from a region contaminated by YLYEIAR.

As the concentration of Y_5R increased by a factor of ten from tissue A to tissue B, $\sum_i I_i([P+H]^+)$ increased only by a factor of 4.3 (p value of 3×10^{-14}). In contrast, $\sum_i\{I_i([P+H]^+)/I_i([M+H]^+)\}$ increased in proportion to the peptide concentration (p = 0.61). We also performed similar experiments for another tissue, to be called tissue C, which was intentionally contaminated as follows. We cleaned a tissue by Procedure II, loaded 4 μL of a solution containing 200 pmol of YLYEIAR at one edge, dried it, spray-coated it with a solution containing 25 nmol of CHCA and 1.5 pmol of Y_5R per μL, and took the MALDI spectra at several spots in the contaminated region. Here, Y_5R is playing the role of the analyte while YLYEIAR is playing that of a contaminant. From the sets of spectra we acquired, we evaluated $\sum_i I_i([P+H]^+)$ and $\sum_i\{I_i([P+H]^+)/I_i([M+H]^+)\}$ for Y_5R. Their averages are listed in Table 2.2. The peptide-to-matrix ion abundance ratios measured for tissues A and C are similar (p = 0.21) while the total peptide ion abundances are not ($p = 1 \times 10^{-17}$). The above data suggest that the ion abundance ratio is a good representation of the peptide concentration at any location on a tissue while the peptide ion abundance is not.

Image distortion due to matrix suppression. To observe the influence of matrix suppression on MALDI image maps, we performed the following two

experiments for Y_5R on tissue samples. In the first experiment, Y_5R and YLYEIAR were taken as the analyte and the contaminant, respectively. The method to prepare a tissue sample is as follows. We cleaned a tissue by Procedure II and contaminated it by loading 4 μL of a solution containing 200 pmol of YLYEIAR at one (bottom) edge of the tissue and the same volume of a solution containing 600 pmol of the same peptide at the opposite (top) edge. Each volume spread out to a circle with around 2 mm in diameter. After the solvent had evaporated, the tissue surface was spray-coated with a solution containing 1.5 pmol of Y_5R and 25 nmol of CHCA per μL. MALDI spectra acquired under the TIC control from spots near the bottom (lightly contaminated) and top (heavily contaminated) edges are shown in Figures 2.1(c) and 2.1(d), respectively. Comparing Figures 2.1(a) and 2.1(c), one finds that the matrix suppression by YLYEIAR somewhat reduces the abundances of all the matrix-derived ions. However, the matrix suppression near the bottom edge is not severe, only around 60%. In contrast, all the CHCA-derived ions become very weak in Figure 2.1(d). Dominant ions in this spectrum are mostly YLYEIAR-derived. The matrix suppression in Figure 2.1(d) estimated from the abundances of $[CHCA + H]^+$ in Figures 2.1(a) and 2.1(d) is 95%, which is larger than our guideline of 70%.

In Figure 2.2(a), a color-coded image map constructed with the peptide ion abundances ($\sum_i I_i([P + H]^+)$) measured at many spots on the tissue is shown. The peptide ion abundance at each spot was normalized to the largest value observed. A similar map constructed with the peptide-to-matrix ion abundance ratio is shown in Figure 2.2(b). Finally, a matrix suppression map (eqn. (2.2)) is shown in Figure 2.2(c). In this figure, the matrix suppression near the top edge is larger than in the bottom edge, as mentioned above.

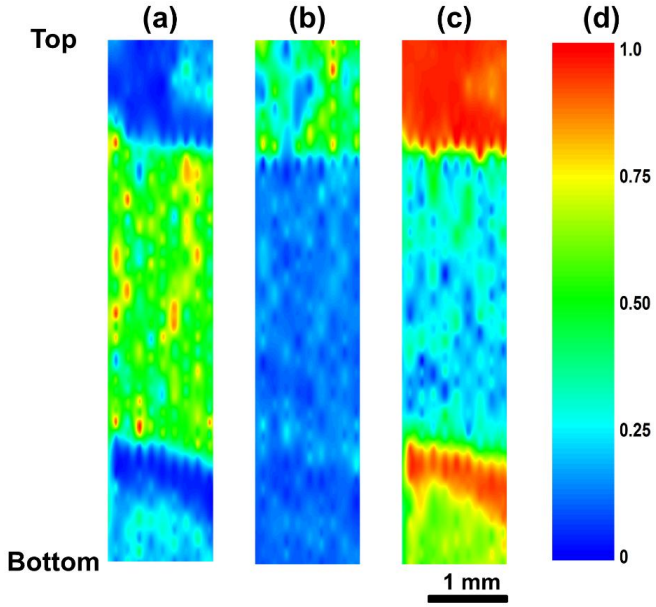

Figure 2.2 Image maps of Y_5R on a tissue that was spray-coated with a solution containing CHCA and Y_5R. The tissue was contaminated by larger (near the top edge) and smaller (near the bottom edge) amounts of YLYEIAR. Image maps were constructed with (a) $\sum_i I_i([P+H]^+)$ and (b) $\sum_i\{I_i([P+H]^+)/I_i([M+H]^+)\}$. (c) is the suppression (eqn. (2.2)) map. To draw (a), $\sum_i I_i([P+H]^+)$ at each spot was normalized to the largest value in the map and color-coded according to the scale in (d). (b) was drawn similarly. To draw (c), matrix suppression at each spot was color-coded to the scale in (d).

The image map for Y_5R constructed with the peptide ion abundance, Figure 2.2(a), indicates that the tissue is roughly divided into three parts, top, middle, and bottom, that have small, medium, and small amounts of Y_5R, respectively. This is in disagreement with our expectation that the concentration of Y_5R would be the same throughout the sample. In the image map constructed with the peptide-to-matrix ion abundance ratio, Figure 2.2(b), the amount of Y_5R in the bottom part becomes comparable to that in the middle part, in agreement with our expectation. On the other hand, the amount of Y_5R in the top part appears larger than in the other parts, in disagreement with our expectation. Looking at the suppression map in Figure 2.2(c), however, one realizes that the image distortion in the top part has arisen due to high matrix suppression—depending on the peptide analyzed, the peptide-to-matrix ion abundance ratio can be larger or smaller than the correct value (ref. 48).

Matrix suppression by materials originating from the tissue can also distort an image map. Amounts of such materials in a sample may vary depending on the cleaning procedure used. In our second experiment, we first cleaned a tissue by Procedure I. Then, one part (bottom) of the tissue was dipped twice in 100% ethanol for 30 seconds. That is, the bottom part of

the tissue was cleaned by Procedure II while the top part was cleaned by Procedure I. At the top edge of the tissue, we loaded 6 μL of a solution containing 100 pmol of Y_5R. Then, we spray-coated the whole tissue with a solution containing 25 nmol of CHCA and 1.5 pmol of Y_5R per μL. In the matrix suppression map, Figure 2.3(c), drawn from the spectral data acquired for this sample, matrix suppression near the top part is 50-90%, which is larger than 5-40% near the bottom part, as expected.

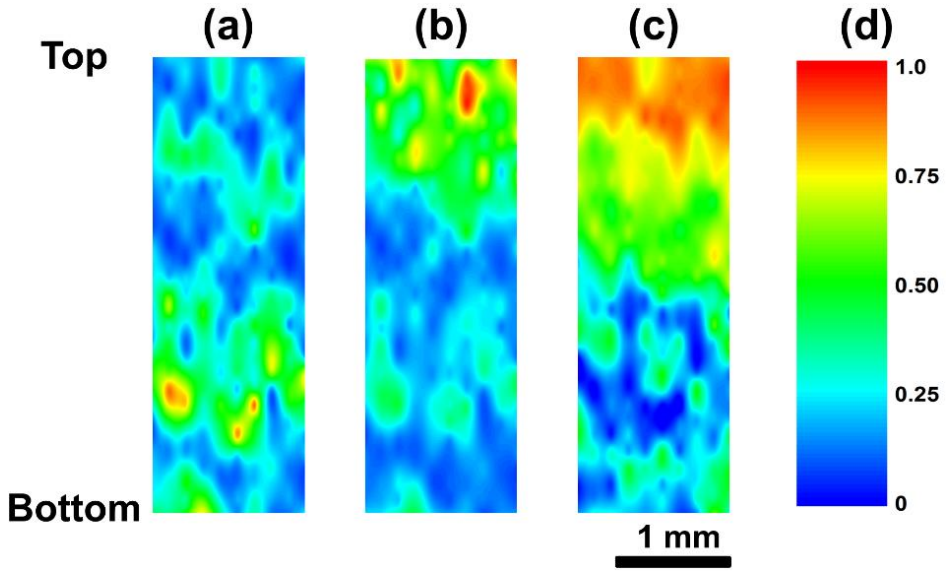

Figure 2.3 Influence of the tissue cleaning procedure on the image map of Y_5R. The top and bottom parts of a tissue were cleaned by Procedures I and II, respectively. 6 μL of a solution containing 100 pmol of Y_5R was loaded near the top edge. Finally, the whole tissue was spray-coated with a solution containing 1.5 pmol of Y_5R and 25 nmol of CHCA per μL. (a) and (b) are image maps constructed with $\sum_i I_i([P+H]^+)$ and $\sum_i\{I_i([P+H]^+)/I_i([M+H]^+)\}$, respectively. (c) is the suppression map. (d) shows the scale used in color-coding.

The image map constructed with the peptide ion abundance, Figure 2.3(a), indicates that the concentration of Y_5R in the top part is smaller than that in the bottom part. This is in disagreement with our expectation. In contrast, the image map constructed with the peptide-to-matrix ion abundance ratio, Figure 2.3(b), predicts higher concentration of Y_5R near the top edge, which is likely because the matrix suppression near the top part is mostly smaller than 70%. That is, the suppression map constructed with the imaging data can be a useful guideline to check the relative quantitativeness of the image map.

2.4 Conclusion

Although MALDI imaging is a powerful technique for visualizing the presence of certain materials at particular locations on a tissue, a method to construct a quantitatively meaningful image map from experimental data is not available yet. In this work, we demonstrated that such maps could be constructed by adopting the peptide-to-matrix ion abundance ratio as the measure of the analyte concentration at the spot rather than the analyte ion abundance itself. Acquisition of spectral data at a fixed effective temperature was one of the requirements. Even the peptide-to-matrix ion abundance ratio might not be a reliable measure of the peptide concentration in the region where the sample is heavily contaminated by salts and/or by bases. Then, the matrix suppression map drawn from imaging data can be a useful guideline to check the quantitative reliability of the image map. We may enhance the relative quantitativeness of the map through a reduction of the matrix suppression by cleaning the tissue or by diluting the analyte.

Chapter 3

Discovery of a solvent effect preventing quantitative profiling by MALDI and its treatment

3.1 Introduction

Measuring the distribution of a substance, i.e., profiling or imaging, in a biological sample is an important technical subject in biology.[34-38,56-57,28] Mass spectrometric profiling using ion signals generated by matrix-assisted laser desorption ionization (MALDI), or MALDI profiling,[38,28] is particularly attractive owing to its excellent sensitivity, ability to identify substances, and tolerance to impurities in biological samples.

The first concern in profiling is to identify the analytes present at a particular location on the sample. Determining their distributions over

multiple locations then becomes the next concern. Determining the absolute amount of an analyte, or absolute quantification,[13,29] at each location is a formidable task. In most cases, even determining the relative amounts of an analyte at different locations, i.e., relative quantification,[13] is difficult as well. Accordingly, one may have to be content with information about which of the two locations has more of the analyte of interest. Although this is another kind of relative quantification, we will refer to this as a large-or-small analysis.

In general, MALDI is not regarded as a quantitative tool because the ion signals generated by MALDI are usually irreproducible.[13,45,23] Recently,[23] however, we found that they became eproducible when a sample is homogeneous and when the temperature in the early plume (T_{early})[28] where the in-source decay[60] occurs is fixed. We developed a technique to fix T_{early} (see the Experimental section).[51] We also found that the analyte-to-matrix ion abundance ratio in a spectrum, $I([A + H]^+)/I([M + H]^+)$, was proportional to the neutral ratio in the solid sample, A/M.[12] Here, $I([A + H]^+)/I([M + H]^+)$ and A/M are termed the ion ratio and the analyte concentration, respectively. We used a plot of the ion ratio versus the analyte concentration as the calibration curve for analyte quantification.[48] Also, we defined the matrix

suppression (S)[49] as $1 - I([M + H]^+)/I_0([M + H]^+)$, and $I_0([M + H]^+)$ and $I([M + H]^+)$ represent the matrix ion abundances in the spectrum of a pure matrix and of a matrix-analyte mixture, respectively. The calibration curve deviated from linearity when S exceeded a critical value.[49] That is, even the large-or-small information based on ion abundances is erroneous unless the analysis is made carefully.[43]

In our previously published study of the utility of our method for analyte quantification in profiling, we analyzed samples with known concentrations of an analyte in the matrix layer.[61] For accurate results, we prepared a solution containing both a matrix and an analyte, loaded it onto a clean tissue, and dried the tissue. We refer to this as the premixed sample preparation process. We quantified the analytes in premixed samples using this method and observed excellent agreement with the prepared concentrations.

However, premixed sample preparation is not how a sample is pretreated for a profiling experiment. Here, the analyte is present in the sample from the beginning and a solution containing the matrix is put onto the sample surface and dried.[62,63] During this process, there is no guarantee that all of the analytes in the original sample will be transferred to the matrix layer.[63] To check this, we devised a stepwise sample preparation method in which the

analyte and matrix solutions were loaded and dried one after another. Using this method, we observed that as the water contents of the mixed solvents used to prepare matrix solutions got lower, the quantification results for analytes became smaller than the prepared amounts. The origin of the discrepancy, which turned out to be a kind of solvent effect, is presented together with remedies in this paper.

3.2 EXPERIMENTAL

The apparatus used in this work is a home-built MALDI-TOF (time-of-flight)[26] It consists of an ion source with delayed extraction, an ion gate, a reflectron, and a microchannel plate detector. Pulsed output of a nitrogen laser (MNL100, Lasertechnik Berlin, Berlin, Germany) at 337 nm is used to induce MALDI.

All spectra were acquired at a fixed T_{early} by controlling the total ion count (TIC).[51] The TIC represents the total number of the analyte- and matrix-derived ions in a spectrum. For each measurement at a spot, we averaged the spectra over ten consecutive laser shots, measured the TIC, changed the pulse energy to keep the TIC constant, and resumed the spectral acquisition process. Spectral acquisition at a spot continued until the spot was nearly depleted. In practice, we began spectral acquisition at two times the threshold pulse energy and ended when it reached three times the threshold.

We took the sum of the spectra acquired at each spot, evaluated the ion ratio in the summed spectrum, and multiplied it by the number of spectra taken from the spot. The result is called the total ion ratio. According to our previous study, the total ion ratio is proportional to the total amount of the

analyte at the spot.[61,64]

Sample preparation: In the stepwise method devised to mimic the sample pretreatment for profiling, first we produced an analyte spot with a circular cross section (200 μm in diameter) on a metallic sample plate using an inkjet printer.[65] A circular matrix layer was then prepared at the same location using the same printer. Initially, we used an inkjet printer (μMatrix Spotter, ASTA, Suwon, Korea) that emitted a liquid jet at a fixed volume (3 pL per droplet). In the subsequent study conducted to explain the discrepancies in the quantification results, a different inkjet printer was used (CHIP-1000, Shimadzu, Kyoto, Japan). This second printer was more versatile than the first in various aspects. Concerning the present study, the most important aspect was that the volume of a liquid jet droplet was controllable, with a minimum of ~100 pL. The stepwise methods using the two inkjet printers will be differentiated by the corresponding notations stepwise-μSpotter and stepwise-CHIP1000. The amounts of the matrix and the analyte loaded onto a sample plate were calibrated by UV/VIS spectrophotometry. The volumes of the liquid jets were calibrated similarly.

We also prepared solid samples using premixed solutions, i.e., those containing both a matrix and an analyte. They were used to acquire reference

data, calibration curves in particular. Use of the two inkjet printers here will be differentiated by the notations premixed-μSpotter and premixed-CHIP1000. α-cyano-4-hydroxycinnamic acid (CHCA) and 2,5-dihydroxybenzoic acid (DHB) were used as the matrix. For solid samples using CHCA as the matrix, the conventional method of loading a premixed solution with a pipet and then vacuum-drying it was also used, referred to here as premixed-pipet. The notation CHCA-premixed-pipet represents the preparation of a sample containing CHCA as the matrix.

Mixtures of ethanol (EtOH) and water were used as solvents in the stepwise preparation of solutions containing CHCA as the matrix. We also used mixed solvents containing acetonitrile (ACN) or methanol (MeOH) instead of EtOH. For example, 25% ACN in water was used for CHCA-premixed-pipet. We will denote this experimental condition as CHCA-premixed-pipet-ACN/H_2O(25/75). The use of solvents with a water content level greater than 80% or less than 70% produced inhomogeneous samples. During the preparation of samples with CHCA using either of the inkjet printers, EtOH/H_2O(80/20) was used. In this case, the use of a solvent with a water content level greater than 20% clogged the inkjet printer. In the case of DHB, premixed-pipet did not produce a homogeneous sample. When DHB

samples were prepared using either of the inkjet printers, the ethanol content in the water could be changed in the range of 20-80%, as clogging did not occur. Water was the solvent during the preparation of the analyte (Y_5R) solutions. All of the solutions contained 0.1% trifluoroacetic acid.

Peptide Y_5R was purchased from Peptron (Daejeon, Korea). All of the other chemicals were purchased from Sigma (St. Louis, MO, USA).

3.3 RESULTS AND DISCUSSION

During the pretreatment of a sample for profiling, a solution containing a matrix is loaded onto the sample surface to extract an analyte(s) from the sample. In this work, we attempted to investigate the analyte transfer process during this step by studying samples prepared by the stepwise loading-drying of solutions containing an analyte and a matrix. We will first present the calibration curves used to quantify the analytes. The efficiency of the analyte transfer will be presented thereafter.

Calibration curves: Previously, we acquired the calibration curve of the peptide Y_5R in CHCA using samples prepared with premixed-pipet-ACN/H_2O(25/75).[48] 1.0 μL of each premixed solution contained various amounts of Y_5R and 25 nmol of CHCA. In the present work, we acquired the calibration curve under the same condition. The result drawn on the log-log scale is shown in Figure 3.1(a). The slope of 1.04, which is close to 1.0, indicates that the total ion ratio is proportional to the analyte concentration over a wide range of analyte concentrations. The curve shown in Figure 3.1(a) is essentially identical to that in the previous report. We would like to reiterate our claim in the previous report[66] that the calibration curve was insensitive to changes in various experimental conditions such as the

instrument used and its tuning and the solvent in the sample solution. Also, as was observed for Y_5K in CHCA,[66] we expect that the calibration curve constructed using spectral data for samples prepared by premixed-inkjet is identical to that acquired by premixed-pipet. To verify this, we constructed the calibration curves for Y_5R in CHCA prepared by premixed-μSpotter-EtOH/H_2O(80/20) and by premixed-CHIP1000-EtOH/H_2O(80/20). These curves are shown in Figures 3.1(b) and 3.1(c), respectively. The three calibration curves are nearly identical, indicating that an analyte in a matrix can be quantified using a calibration curve constructed for premixed samples prepared in any way one chooses.

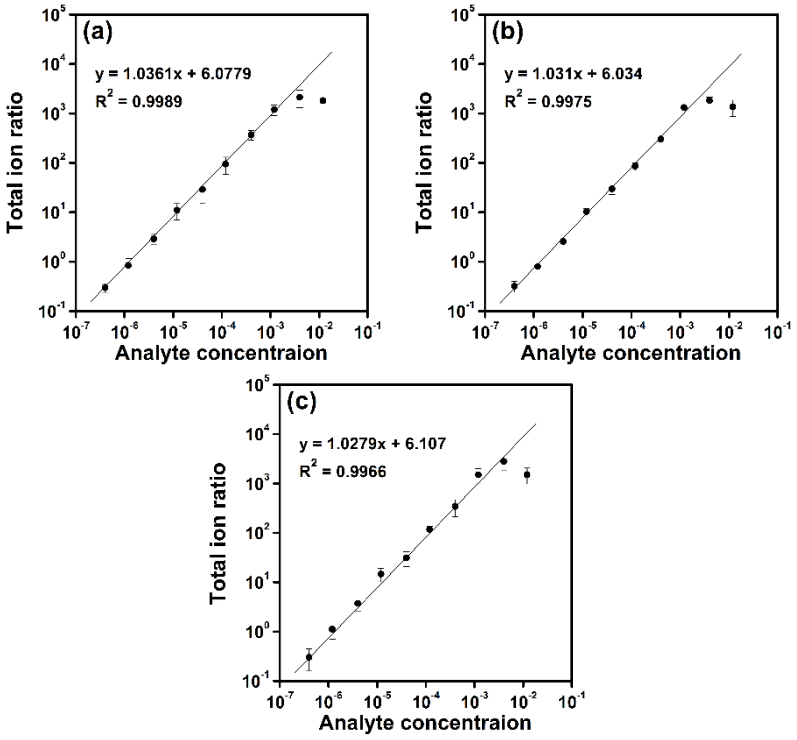

Figure 3.1 Log-log plots of the calibration curves, the total ion ratio vs. the analyte concentration, for Y_5R in CHCA constructed with MALDI data for samples prepared by (a) premixed-pipet-ACN/H_2O(25/75), (b) premixed-μSpotter-EtOH/H_2O(80/20), and (c) premixed-CHIP1000-EtOH/H_2O(80/20). TIC of each spectrum was controlled at 1200.

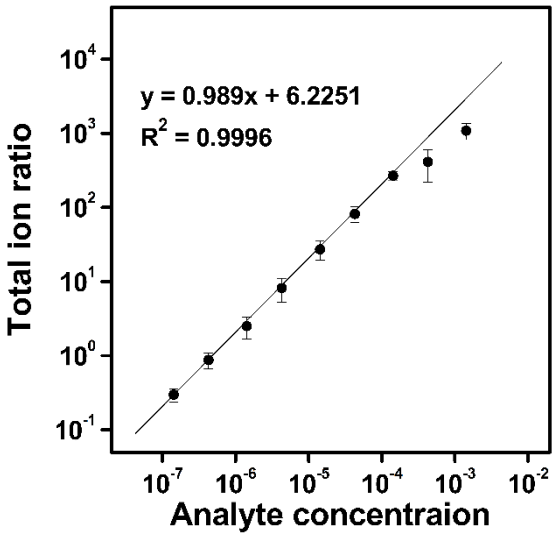

Figure 3.2 Log-log plot of the calibration curve, the total ion ratio vs. the analyte concentration, for Y_5R in DHB constructed with MALDI data for samples prepared by premixed-μSpotter-EtOH/H_2O(20/80).

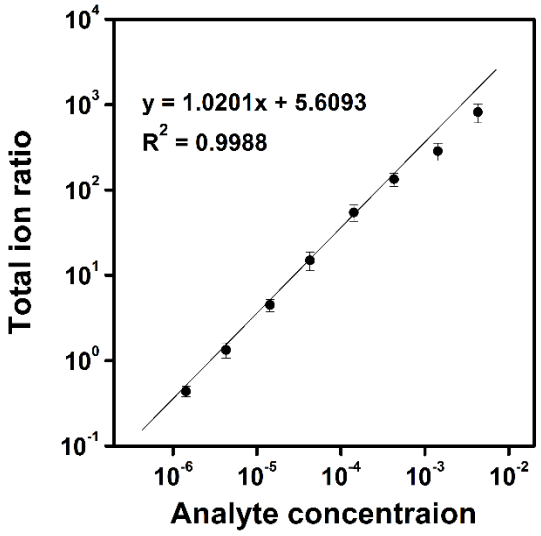

Figure 3.3 Log-log plot of the calibration curve, the total ion ratio vs. the analyte concentration of imipramine in 700 pmol of DHB constructed with MALDI data for samples prepared by premixed-μSpotter-EtOH/H_2O(20/80).

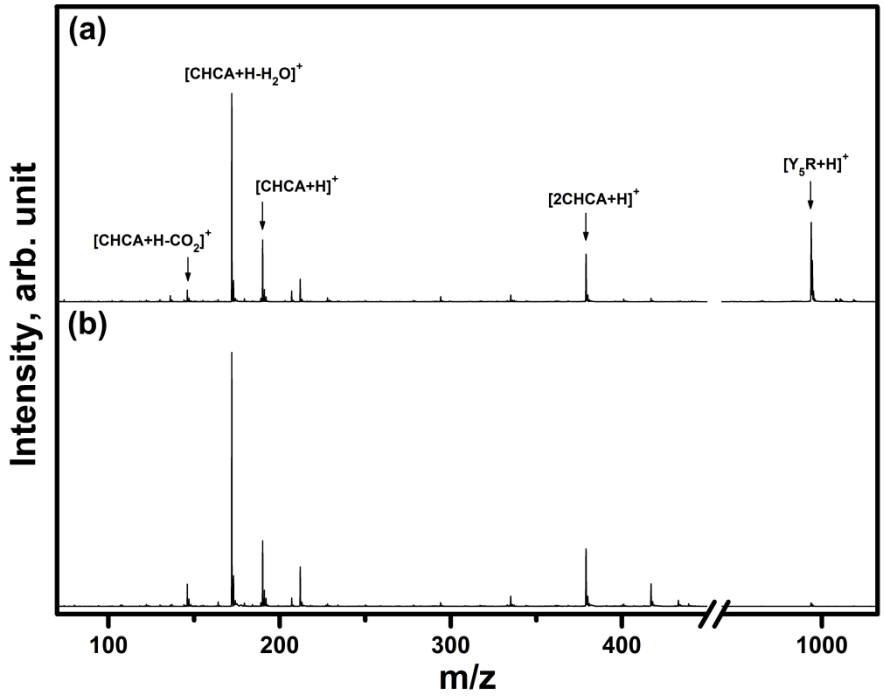

Figure 3.4 Raw MALDI spectra of samples with circular cross section (200 μm o.d.) containing 30 fmol of Y_5R in 250 pmol of CHCA prepared by (a) premixed-μSpotter-EtOH/H_2O(80/20) and (b) stepwise-μSpotter-EtOH/H_2O(80/20). TIC of each spectrum was controlled at 1200.

We will use the calibration curve acquired by premixed-μSpotter-EtOH/H_2O(80/20) for the quantification of Y_5R in CHCA.

For Y_5R in DHB, we acquired the calibration curve using the samples prepared by premixed-μSpotter-EtOH/H_2O(20/80). We did not use EtOH/H_2O(80/20) as the solvent in this case because the samples thus prepared were often inhomogeneous. The calibration curve for Y_5R in DHB is shown in the Figure 3.2. We also constructed the calibration curve for imipramine in DHB using the samples prepared by premixed-μSpotter-EtOH/H_2O(20/80). This is also shown in the Figure 3.3.

Solvent dependence in the quantification of analytes in samples prepared by stepwise-μSpotter: In the initial stage of our study of the sample-to-matrix analyte transfer process, we prepared a circular spot of Y_5R (200 μm in o.d.) on a metal target using the μMatrix Spotter. Then, a layer of CHCA was prepared on the same spot by μSpotter-EtOH/H_2O(80/20). In Figure 3.4, the MALDI spectrum of the stepwise sample containing 30 fmol of Y_5R and 250 pmol of CHCA is shown together with that of the premixed sample with the same overall analyte concentration. It is remarkable to note that the abundance of $[Y_5R + H]^+$ in the spectrum of the stepwise sample is much lower than that of the premixed case. Quantification of Y_5R in the

stepwise sample using the calibration curve in Figure 3.1 resulted in 2±1 fmol of Y_5R, which is 7% of the correct overall concentration. When we changed the solvent to 100% EtOH, a similarly erroneous result of 0.9±0.2 fmol of Y_5R was obtained. The data indicated that Y_5R was not efficiently transferred to the matrix layer when using samples prepared by stepwise-μSpotter-EtOH/H_2O(80/20), presumably due to a solvent effect (see below) which arises during the transfer of the analyte. We could not repeat the CHCA-MALDI experiment with different solvents because use of a solvent with a water content level higher than 20% clogged the μMatrix Spotter.

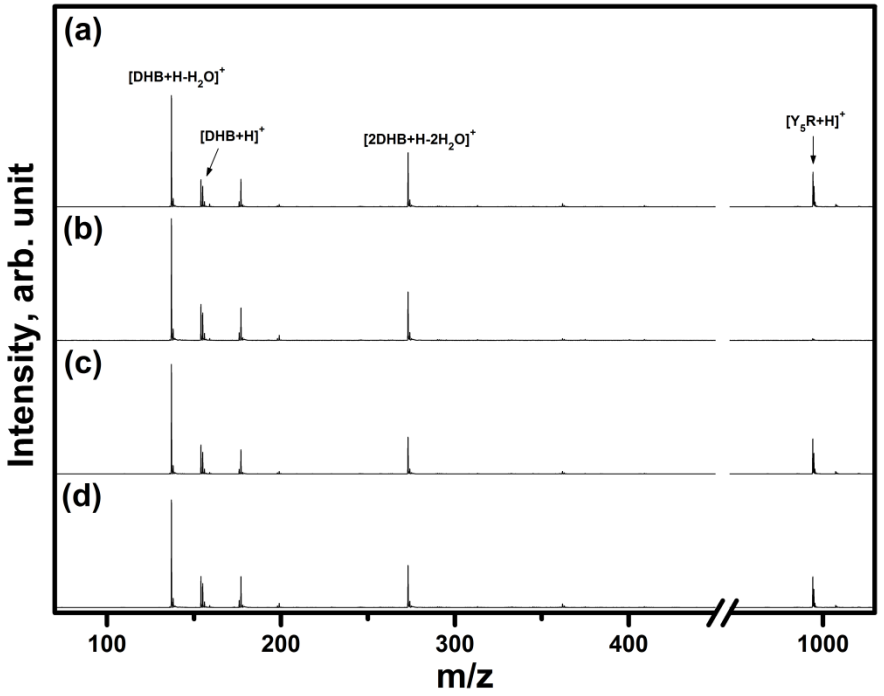

Figure 3.5 Raw MALDI spectra of samples with circular cross section (200 μm o.d.) ontaining 30 fmol of Y_5R in 700 pmol of DHB prepared by (a) premixed-μSpotter-EtOH/H_2O(80/20), (b) stepwise-μSpotter-EtOH/H_2O(80/20), (c) premixed-μSpotter-EtOH/H_2O(20/80), and (d) stepwise-μSpotter-EtOH/H_2O(20/80). TIC of each spectrum was controlled at 1200.

Table 3.1 Quantified amounts of Y_5R in 700 pmol of DHB prepared by stepwise-μSpotter

Correct amount , in fmol	Quantified amount , in fmol	
	$EtOH/H_2O(80/20)$	$EtOH/H_2O(20/80)$
1.0	0.6 ± 0.3	0.9 ± 0.2
3.0	1.0 ± 0.4	2.7 ± 0.8
10	1.8 ± 0.9	9.5 ± 2.6
30	1.3 ± 0.5	32 ± 8.1

Correct amount , in fmol	Quantified amount , in fmol	
	$MeOH/H_2O(80/20)$	$MeOH/H_2O(20/80)$
1.0	1.2 ± 0.5	1.0 ± 0.3
3.0	1.5 ± 0.3	2.8 ± 1.1
10	1.9 ± 0.5	11 ± 3.8
30	2.0 ± 0.7	27 ± 6.7

Correct amount , in fmol	Quantified amount , in fmol	
	$ACN/H_2O(80/20)$	$ACN/H_2O(20/80)$
1.0	0.6 ± 0.2	0.7 ± 0.3
3.0	0.5 ± 0.2	3.4 ± 1.1
10	1.9 ± 0.8	8.5 ± 3.8
30	4.5 ± 1.9	29 ± 11

Table 3.2 Quantified amounts of imipramine in 700 pmol of DHB prepared by stepwise-μSpotter with various solvents

Correct amount , in fmol	Quantified amount , in fmol	
	$EtOH/H_2O(80/20)$	$EtOH/H_2O(20/80)$
3.0	3.2 ± 1.9	3.8 ± 1.3
10	6.3 ± 3.7	10 ± 4
30	7.1 ± 3.5	32 ± 11

Correct amount , in fmol	Quantified amount , in fmol	
	$MeOH/H_2O(80/20)$	$MeOH/H_2O(20/80)$
3.0	0.6 ± 0.2	2.7 ± 1.0
10	6.6 ± 2.3	13 ± 5
30	12 ± 6	27 ± 6

Correct amount , in fmol	Quantified amount , in fmol	
	$ACN/H_2O(80/20)$	$ACN/H_2O(20/80)$
3.0	1.1 ± 0.3	3.5 ± 1.7
10	6.6 ± 3.5	8.1 ± 1.7
30	8.6 ± 4.3	31 ± 12

To avoid this difficulty, we decided to study the phenomenon using DHB as the matrix, which dissolves well in various solvents.

The DHB-MALDI spectra of Y_5R samples prepared by various methods are shown in Figure 3.5. In all cases, the overall amounts of Y_5R and DHB were 30 fmol and 700 pmol, respectively. Because the abundances of $[DHB + H]^+$ in the four spectra are similar, the concentration of Y_5R in the matrix layer of each sample will be nearly proportional to the abundance of $[Y_5R + H]^+$ in each spectrum. Figures 3.5(a) and 3.5(b) show the spectra of samples prepared by premixed-μSpotter-EtOH/H_2O(80/20) and by stepwise-μSpotter-EtOH/H_2O(80/20), respectively. Compared to the abundance of $[Y_5R + H]^+$ in Figure 3.5(a), that of the same ion in Figure 3.5(b) is much lower. This is the same trend as observed for CHCA. The quantification results for Y_5R in the two samples were 33 and 1.5 fmol. Compared to the prepared amount of 30 fmol, the quantified amount of 33 fmol is a reasonable value whereas 1.5 fmol is too low. The results for various amounts of Y_5R in DHB prepared by stepwise-μSpotter-EtOH/H_2O(80/20) and stepwise-μSpotter-EtOH/H_2O(20/80) are listed in Table 3.1.

Figures 3.5(c) and 3.5(d) show the spectra of samples prepared with relatively more water in the solvent, i.e., premixed-μSpotter-

EtOH/H_2O(20/80) and stepwise-μSpotter-EtOH/H_2O(20/80), respectively. It is to be noted that the matrix ion abundances are similar in the two spectra. In addition, the abundances of $[Y_5R+ H]^+$ in the two spectra are also similar. These indicate similar concentrations of Y_5R in the two samples. In fact, the quantification results were 31 and 32 fmol of Y_5R, respectively. (more comprehensive data is given in the Table 3.1. We made similar measurements for stepwise samples of Y_5R prepared with MeOH/H_2O(80/20), MeOH/H_2O(20/80), ACN/H_2O(80/20), and ACN/H_2O(20/80). These results are listed in the Table 3.1, where they are shown to be similar to those obtained with EtOH/H_2O as the solvent. We also made similar measurements for the DHB-MALDI of imipramine using the same six combinations of solvents. These results are also listed in Table 3.2; they are nearly identical to those for Y_5R.

To summarize, the sample-to-matrix analyte transfer efficiency was poor when a sample was pretreated by stepwise-μSpotter-X/H_2O(80/20) (X = ACN, EtOH, or MeOH), whereas a nearly complete transfer occurred upon a pretreatment by stepwise-μSpotter-X/H_2O(20/80). The same held true for CHCA- and DHB-MALDI and for the two analytes we thoroughly tested, i.e., Y_5R and imipramine. In short, the water content in the solvent of the matrix

solution was responsible for the discrepancies in the quantification results observed in this work.

One may attribute the solvent effect summarized above to various possibilities. First, this solvent effect may manifest if the solubility of an analyte in a solvent decreases significantly when the water content decreases. This explanation is unlikely, however, because the analytes used here dissolve well even in pure EtOH. Second, the analytes may somehow not be easily incorporated into the matrix crystal as the water content of the solvent decreases. This is not likely either, as the DHB-MALDI of the analytes is efficient regardless of the composition of the solvent used in the premixed preparation of the samples.

In addition to the conventional manifestations of the solvent effect mentioned above, another factor which can arise during the sample pretreatment process can affect the efficiency of the analyte transfer. This is the contact time between the sample surface and a droplet of the matrix solution that has been deposited onto the sample surface. As the solvent becomes more polar, the droplet will evaporate more slowly. Alternatively, as the water content of a solvent increases, the surface tension of a solvent drop increases, which may result in a longer evaporation time for the drop. Then,

a longer evaporation time would allow a longer contact time between the sample and the matrix solution. This may result in more efficient analyte extraction.[67,68] As a rough check of the feasibility of this idea, we loaded 1.0 μL each of EtOH/H_2O(80/20) and EtOH/H_2O(20/80) onto a metal plate and measured the decrease of their masses as a function of time. Their half-lives under the room condition were ~60 and ~200 s, respectively. The same measurement carried out with 10 μL of the solvents showed half-lives of ~100 and ~1000 s, respectively. Hence, it is clear that it takes noticeably more time for a droplet of EtOH/H_2O(20/80) to evaporate as compared to that required for a droplet of EtOH/H_2O(80/20). This provides a partial explanation of the solvent effect encountered here. Another way to increase the sample-solvent contact time is to use a larger liquid jet droplet. Such a test could not be done using the μMatrix Spotter because the volume of the liquid droplets emitted by the device was fixed at 3 pL.

Analyte transfer efficiency versus volume of a matrix solution droplet: When using the other inkjet printer, CHIP-1000, we can control the volume of an emitted liquid droplet. The adjustment of the volume of a matrix droplet deposited at a spot was done as follows. We first calibrated the volume of an emitted droplet by UV/VIS spectrophotometry of a solution

containing a known amount of CHCA. This value was ~150 pL for EtOH/H_2O(80/20). We then utilized the capability of CHIP-1000 to consecutively emit many droplets at a time. These consecutive droplets arrive at a spot on a sample virtually at the same time. Hence, they can be regarded collectively as one liquid drop with a larger volume, V_d. Because V_d was not proportional to the number of droplets deposited per shot, calibration by UV/VIS spectrophotometry was necessary.

In all of the MALDI experiments carried out to observe the drop-size effect on the transfer efficiency, we first deposited 30 fmol of Y_5R onto a circular spot (200 μm o.d.). Then, we deposited a fixed total volume of a matrix solution with a fixed concentration onto the same circular spot.

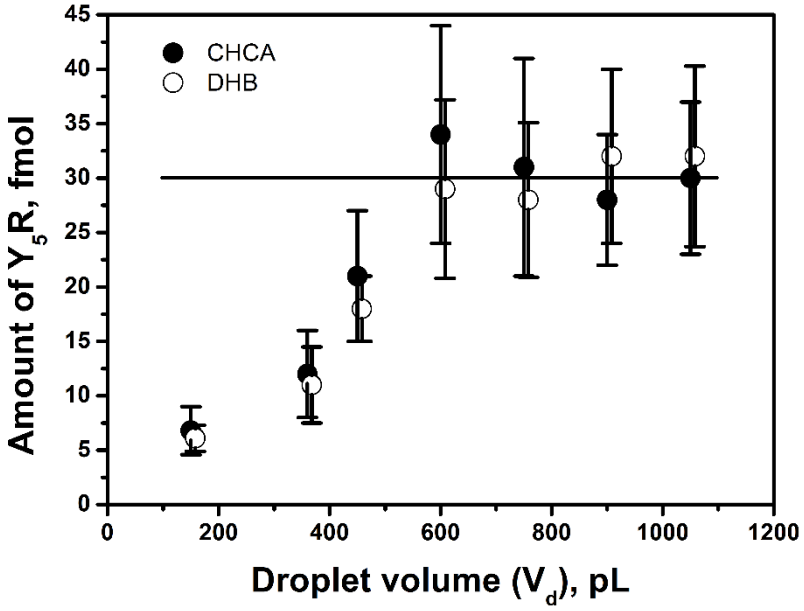

Figure 3.6 The quantified amounts of Y_5R vs. the droplet volume (V_d) in CHCA- and DHB-MALDI of samples prepared by stepwise-CHIP1000-EtOH/H_2O(80/20). CHCA- and DHB-MALDI data are drawn with filled (●) and open (○) circles, respectively. The prepared amount of Y_5R was 30 fmol either in 250 pmol of CHCA or in 700 pmol of DHB, which is drawn as a horizontal line.

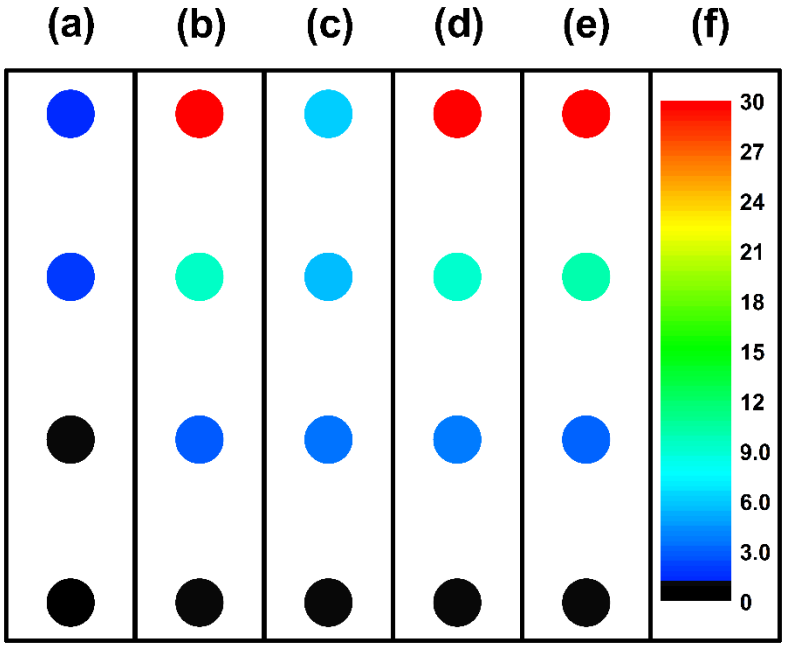

Figure 3.7 Columns (a), (b), (c), and (d) show the color-coded profile maps for the samples of Y_5R in DHB prepared by stepwise-μSpotter-EtOH/H_2O(80/20), stepwise-μSpotter-EtOH/H_2O(20/80), stepwise-CHIP1000-EtOH/H_2O(80/20) with V_d of 150 pL, and stepwise-CHIP1000-EtOH/H_2O(80/20) with V_d of 900 pL, respectively. The prepared ('correct') profile is shown in column (e). The scale for the amount of Y_5R, in number of fmol in 700 pmol of DHB, is drawn in column (f).

Table 3.3 Quantified amounts of Y_5R in 700 pmol of DHB prepared by stepwise-CHIP1000-EtOH/H_2O

Correct amount , in fmol	Quantified amount , in fmol	
	Droplet volume 150 pL	Droplet volume 900 pL
1.0	1.1 ± 0.2	1.1 ± 0.3
3.0	3.4 ± 1.0	3.7 ± 1.1
10	5.4 ± 1.6	9.0 ± 2.3
30	6.1 ± 1.0	32 ± 7.9

In this step, we varied V_d by varying the number of consecutive liquid droplets. When viewed with a microscope in the apparatus, liquid droplets with V_d ~150 pL deposited on the target disappeared rapidly, whereas those with larger V_d values stayed longer, in agreement with our explanation.

The amounts of Y_5R quantified versus V_d in CHCA- and DHB-MALDI are shown in Figure 3.6. It should be noted that the quantified amounts increase steadily as V_d increases. Eventually at a V_d value of 600 pL, the quantification results approach the correct amounts of 30 fmol. The transfer efficiencies observed in CHCA- and DHB-MALDIs tend to change similarly to the change of V_d, providing strong evidence that the observed discrepancies are unrelated to the matrix used.

Profiling of Y_5R by DHB-MALDI: We acquired quantification results for samples containing 1-30 fmol of Y_5R prepared by various methods. Among these data, those acquired by stepwise-μSpotter-EtOH/H_2O(80/20) and by stepwise-μSpotter-EtOH/H_2O(20/80) are shown in Table 3.1. In addition, two sets of data acquired by stepwise-CHIP1000-EtOH/H_2O(80/20), one produced with a V_d value of 150 pL and the other with that of 900 pL, are shown in Table 3.3.

In Figure 3.7, these data are presented in the form of color-coded profile

maps. Also shown in the figure is a profile plot of the correct amounts, i.e., the results for samples prepared by premixed-μSpotter-EtOH/H_2O(20/80). The figure clearly demonstrates that the water content of the solvent used to extract an analyte(s) from a sample can critically affect the quantitativeness of the analyte profile. It also shows that the above problem can sometimes be avoided by increasing the volume of the matrix solution droplet.

3.4 CONCLUSIONS

Two of the requirements for the quantitative profiling of an analyte in a sample by MALDI are a quantitative sample-to-matrix analyte transfer and the capability of quantifying an analyte incorporated inside a solid matrix. Recently, we developed a method which facilitates the second requirement.[61]

Concerning the first requirement, we found in this work that the use of a matrix solution with a low water content level resulted in a poor sample-to-matrix analyte transfer. We could avoid this negative solvent effect with a more polar solvent or by increasing the size of the matrix solution droplet deposited by a printer. Based on these observations, we suggest that the aforementioned solvent effect arises because the evaporation time of a liquid droplet decreases as the solvent becomes less polar.

Even when the two requirements for quantitative profiling are met, a profiling result still may not be quantitative if the analyte transfer from the bulk of a sample to its surface, and eventually to the matrix layer, does not occur efficiently. This can be particularly troublesome during the profiling of analytes in biological samples. A thorough investigation of this process is therefore needed.

Chapter 4

Quantitative transfer of polar analytes on a solid surface to a liquid matrix in MALDI profiling

4.1 Introduction

Determining the distribution of an analyte(s) on a solid sample with a low (profiling) or high (imaging) spatial resolution by matrix-assisted laser desorption ionization (MALDI) is of great current interest.[36-38,45,56-58,69] In a typical profiling experiment,[38,58] a sample is cut into thin slices. A matrix solution is loaded onto the surface of each slice by various spraying and spotting techniques.[69] After the evaporation of the solvent of the matrix solution from a slice, it is subjected to MALDI analysis. Probably the most important information available from a profiling experiment is the presence/absence of a particular material at a certain location on a slice.[38] After the acquisition of such qualitative information, one naturally demands

a knowledge on the amount of each material at each location.

Although profiling/imaging by MALDI has been practiced for nearly twenty years, acquiring quantitative data, absolute or relative, is still recognized as a formidable task.[38,45] The main difficulty lies in the fact that the abundance of an ion produced by MALDI is not reproducible.[13,23,70] Recently, we proposed a thermal explanation for the changes in ion signals in MALDI and reported a method to keep them constant.[23,51] We also suggested that the analyte-to-matrix ion abundance ratio, $[AH^+]/[MH^+]$, in a spectrum is a good measure of the analyte concentration ($c(A) = [A]/[M]$) in the matrix layer.[48]

For convenience, the transfer of an analyte initially present inside a solid sample to the matrix layer may be considered to occur in two steps, i.e., analyte transfer from the inside of the solid to the surface and a transfer from the surface to the matrix layer. Although both steps would affect the overall efficiency of MALDI profiling and hence its quantitativeness, there was scarcely any reports of investigations of the two steps.[68] In a pioneering study on direct tissue imaging, Caprioli et al. reported various practical aspects of sample preparation.[55,67] Compared to other solvents used to prepare a matrix solution, they found that a 50:50 ethanol/water ($EtOH/H_2O$)

produced ion signals from relatively more proteins in a sample, which were stronger at the same time.[67] No explanation of the solvent effect was provided by the authors. However, based on the two-step analyte transfer mentioned above, it is likely that the solvent effect would mainly affect the efficiency of the second step. In our recent study of the profiling of a peptide by MALDI with solid matrixes, i.e., α-cyano-4-hydroxycinnamic acid (CHCA) and 2,5-dihydroxybenzoic acid (DHB), we observed that the surface-to-matrix analyte transfer occurred quantitatively when 20:80 EtOH/H_2O was used.[71] In contrast, the transfer efficiency was poor when 80:20 EtOH/H_2O was used. We found evidence that a longer evaporation time of the 20:80 mixture was responsible for its higher extraction efficiency of the analyte from the sample surface.[71]

Gross et al. found that a room temperature ionic liquid produced by the 1:1 mixing of an acid with a base was a good matrix for the MALDI of polar biological molecules.[72] Materials used as solid MALDI matrixes, such as CHCA and DHB, were adopted as acids, whereas aliphatic or aromatic amines were used as bases. Li and Gross reported linear calibration curves for quantification by MALDI using ionic liquid matrixes, although over limited dynamic ranges.[73] Fournier et al. demonstrated the imaging, although

not quantitative, of lipids in cells by MALDI with ionic liquid matrixes.[74] We reported that a genuinely fluidic liquid could be produced by the nonstoichiometric mixing of the above acids and bases and air-drying of the mixture to eliminate the solvent—in profiling, a solution of liquid matrix in a solvent is loaded and dried.[75] Such a liquid, which is not entirely ionic, remained fluidic, and hence homogeneous, even after prolonged storage inside a vacuum and after extensive bombardment—10000 shots or more—by laser pulses.[75] For MALDI with a solid matrix, the ion signals from a spot changed as the laser irradiation continued.[13,23,70] Hence, a method was needed to make MALDI reproducible. In contrast, we could generate reproducible ion signals without much effort in liquid MALDI,[75] an advantage in quantitative profiling. More importantly, the fact that the liquid matrix remains fluidic over an extended period of time can be an advantage for the efficient extraction of analytes from a solid sample surface. In this work, we checked whether the above potential advantages of a liquid matrix would make liquid MALDI useful for the quantitative profiling of polar analytes.

4.2. Experimental

Acquisition of spectral data: A custom-made MALDI-TOF instrument was used in this work.[26] An important characteristic of the instrument is that the dynamic range of its detection system is wide enough to allow the detection of analyte-derived ions without deflecting matrix-derived ions away. The 337 nm output of a nitrogen laser (MNL100, Lasertechnik Berlin, Berlin, Germany) was used. The laser pulse energy at the MALDI threshold was measured and found to be approximately 0.75 μJ for the matrix used in this work. Spectral acquisition was done at twice this value, i.e., 1.5 μJ. The total number of ions (total ion counts, TIC) produced by MALDI at a spot on a freshly prepared sample was measured. We routinely kept TIC constant throughout the experiment by feedback adjustment of the pulse energy.[51] TIC control is useful for the acquisition of reproducible spectra from a solid sample. Previously, we found that MALDI spectra acquired with a liquid matrix were reproducible even without the TIC control when the top center of a droplet was irradiated by the laser.[75] However, using the TIC control made the experiment easier.

The liquid matrix and reagents: The matrix solution used in this work contained 320 nmol of 3-aminoquinoline (3-AQ) and 40 nmol of CHCA in

1.0 μL of methanol. For simplicity, this matrix solution will be referred to as 3-AQ/CHCA/MeOH. In this work, a tiny aliquot of this solution was loaded onto a sample plate and dried, resulting in an 8:1 mixture of 3-AQ and CHCA—although some MeOH may remain in the mixture, it would further evaporate when the liquid matrix is introduced into the vacuum. This liquid matrix is termed 3-AQ/CHCA. Analyte solutions were also prepared using methanol as a solvent. 1.0 μL of an analyte solution contained 1-100 pmol of an analyte. The matrixes 3-AQ and CHCA and an analyte were purchased from Sigma (St. Louis, MO, USA). Peptide Y_5R was purchased from Peptron (Daejeon, Korea).

Sample preparation: We loaded liquid samples either on hydrophobically coated or on bare metal surfaces of commercial sample plates (ASTA, Suwon, Korea) and found that the former surface provided a better control of the shape of liquid matrix drops.

We first produced an analyte layer with a circular cross-section on the sample plate using either an inkjet printer (μMatrix Spotter, 3 pL per drop) manufactured by ASTA (Suwon, Korea) or another (CHIP-1000, 150 pL per drop) by Shimadzu (Kyoto, Japan). We refer to the above circular cross-section as the analyte circle with radius r_A. The μMatrix Spotter was used to

prepare an analyte circle with a r_A of 1000 μm. In this case, the magnitude of r_A was set by the printer. The CHIP-1000 was used to prepare a smaller analyte circle ($r_A \leq 60$ μm). In this case, the radius of one drop of the analyte solution was taken as r_A.

When a small volume of a matrix solution is loaded above the analyte layer by CHIP-1000 and dried, a liquid matrix drop with a hemispherical shape is produced (see the next section). The circular analyte-matrix contact area will be called a matrix circle with radius r_M. By repeating this process, we can produce a liquid matrix layer with a desired radius. Measurement of r_M will be presented in the next section.

Landing of one drop of a matrix solution on the analyte layer was viewed with a microscope in real time. We approximated the contact region between the analyte layer and the matrix solution drop as a circle and will call it as a matrix solution drop circle with radius r_D. When multiple drops of a matrix solution landed in rapid succession, they merged into a larger drop near the landing position. We used this as a technique to increase the size of r_D. We measured r_D with a photomicroscope in real time.

Samples with three different combinations in the relative sizes of r_A, r_D, and r_M were produced (Figure 4.1). Details of their production and the

quantification results will be presented in the next section. Whenever necessary, we quantified the amounts of the analyte and matrix loaded onto a plate by eluting the sample with methanol and analyzing the eluent with UV/VIS spectrophotometry.

4.3. Results and discussion

In a previous section, we introduced our earlier MALDI study of samples prepared by stepwise loading of analyte and matrix solutions, just as in the present study. The main difference of the present study from the previous one is that a liquid matrix, rather than a solid one, was used. It was found in the previous study that the quantification results approached the correct values as the evaporation time for the solvent in the matrix solution got longer. This provided a motivation for the present study because the evaporation time of a liquid matrix drop was expected to be very long. We will first present the geometrical properties of liquid matrixes prepared in this work.

To see the change in the shape of a liquid matrix drop prepared on a hydrophobic part of a sample plate as a function of its amount, variable numbers of matrix solution drops were loaded and dried. Top and side views of a matrix drop with r_M of 290 μm are shown in Figure 4.1. Its height of 270 μm allows us to approximate its shape as a hemisphere. Earlier, the circular cross section at the bottom of this hemisphere was defined as a matrix circle with radius r_M. To evaluate the amount of an analyte in contact with the matrix circle, we need information on the area (S_M) of the circle. In a typical case, we loaded 31.2 nL of a matrix solution containing 10 nmol of 3-AQ

(and 1.25 nmol of CHCA as well). In this case, the S_M value was 0.0314 mm^2. The r_M and S_M values measured for the geometrical cases dealt with in this work are listed in Table 4.1.

We prepared three types of samples with different relative sizes of r_A, r_D, and r_M, referred to here as case A, case B, and case C. In case A, both r_A and r_D were set to be smaller than r_M (r_A, $r_D < r_M$). In case B, r_A was larger than both r_M and r_D with r_M equal to or larger than r_D ($r_D \leq r_M < r_A$). In case C, r_A was the largest of the three as in case B whereas r_D was intentionally made larger than r_M ($r_M < r_D < r_A$).

Table 4.1 Quantification of Y_5R extracted by 3-AQ/CHCA under the MALDI profiling condition

case A (r_A, $r_D < r_M$)						
Amount of 3-AQ, nmol	r_A, µm	r_D, µm	r_M, µm	S_M, mm^2	Prepared amount[a], pmol	Quantified amount,[b] pmol
10	60	60	100	0.031	0.03	0.03 ± 0.01
10	60	60	100	0.031	0.10	0.12 ± 0.03
10	60	60	100	0.031	0.30	0.33 ± 0.05
10	60	60	100	0.031	1.0	0.91 ± 0.04
case B ($r_D \leq r_M < r_A$)						
Amount of 3-AQ, nmol	r_A, µm	r_D, µm	r_M, µm	S_M, mm^2	Prepared amount[a], pmol	Quantified amount,[b] pmol
2.5	1000	60	60	0.011	0.036	0.030 ± 0.005
10	1000	60	100	0.031	0.10	0.13 ± 0.03
40	1000	60	150	0.071	0.23	0.25 ± 0.08
160	1000	60	210	0.14	0.44	0.50 ± 0.10
case C ($r_M < r_D < r_A$)						
Amount of 3-AQ, nmol	r_A, µm	r_D, µm	r_M, µm	S_M, mm^2	Prepared amount[a], pmol	Quantified amount,[b] pmol
2.5	1000	100	60	0.011	0.036	0.070 ± 0.013

[a]Prepared amount of Y_5R inside the matrix circle

[b]Amount of Y_5R determined by our MALDI-based method.

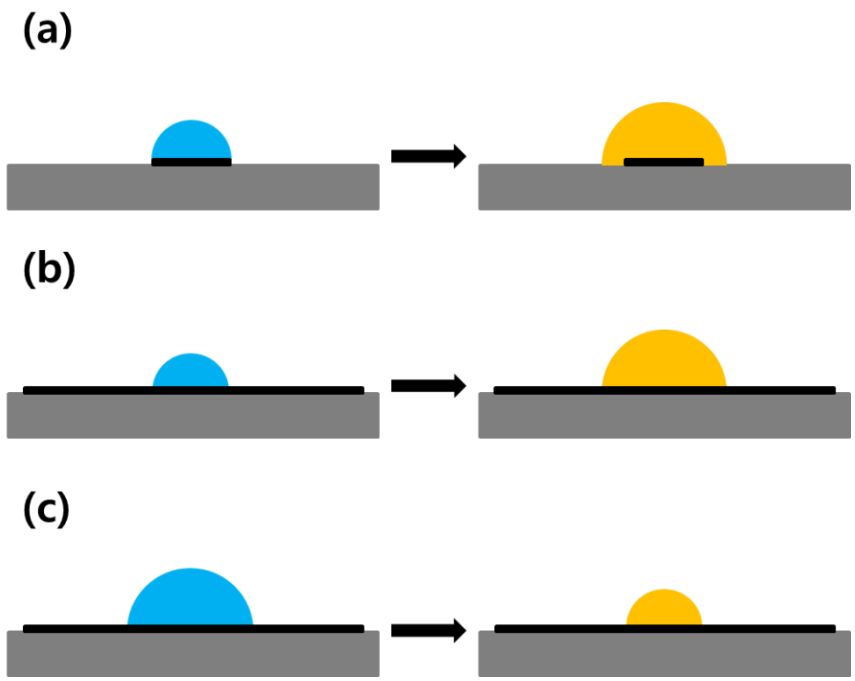

Figure 4.1 Schematic side views of samples drawn for three cases. (a) Case A (r_A, $r_D < r_M$), (b) case B ($r_D \leq r_M < r_A$), and (c) case C ($r_M < r_D < r_A$). The hydrophobically coated sample plate, analyte layer, and matrix layer are drawn in gray, black, and, orange, respectively. Matrix solution drop(s) immediately after landing on the plate, i.e., before solvent evaporation, is (are) drawn in blue. We load as many drops of liquid matrix solution as needed to prepare samples belonging to each case.

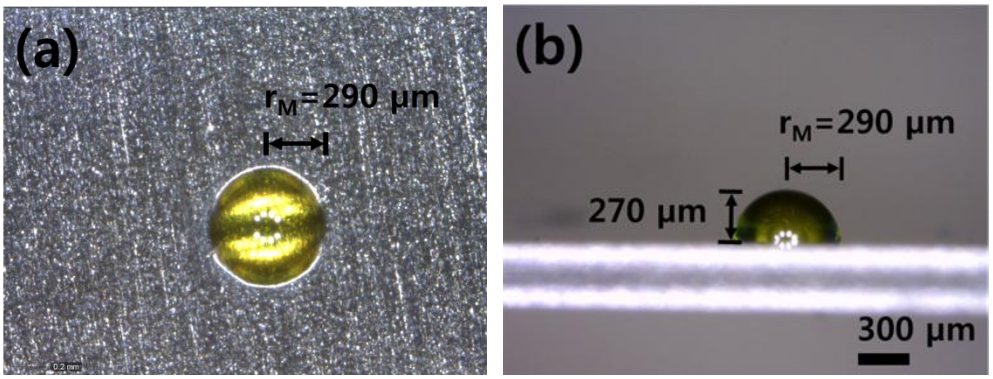

Figure 4.2 Microphotographs of 3-AQ/CHCA prepared on a hydrophobic part of a sample plate. Many drops of a matrix solution, 3-AQ/CHCA/MeOH, were loaded and air-dried. (a) Top view and (b) side view. The radius of the circular cross-section between the sample plate and the matrix, r_M, is marked.

Analyte and matrix circles for the three cases are drawn schematically in Figure 4.1. The samples for cases A and B were prepared by the methods described in the experimental section. Preparation of the samples for case C, making r_D larger than r_M in particular, was somewhat complicated. For ease of the experiment, we decided to use matrix circles with a r_M value of 60 μm. We viewed each drop of the matrix solution (150 pL) arriving at the sample plate with a microscope and found that the drops could be approximated as hemispheres with a r_D of roughly 60 μm. Hence, to ensure that $r_D > r_M$, it was necessary to use matrix solution drops with volumes larger than 150 pL. To do this, we had the CHIP-1000 eject six 150 pL drops of the matrix solution in rapid succession. When viewed with the microscope, the six drops merged into one larger drop with a roughly hemispherical geometry on the sample plate. The radius (r_D) of the solution-plate contact plane was approximately 100 μm. In total, nine cluster shots were made on the plate, loading a total of 2.5 nmol of 3-AQ (and CHCA). After evaporation of the solvent, a matrix circle with a r_M of 60 μm appeared on the plate. The r_A and r_D values of the samples used in the experiments are listed in Table 4.1 together with the r_M and S_M values.

For the quantification of Y_5R transferred to the matrix layer of 3-

AQ/CHCA by our method, we need a calibration curve drawn in the form of $[Y_5RH^+]/[3\text{-}AQH^+]$ vs. the concentration of Y_5R in the matrix.[75] It has been our experience that the calibration curve determined by our method for a given combination of analyte, matrix, and instrument remains valid even a few years after its construction.[66] The calibration curve shown above is essentially the same as the one reported previously.[75] The fact that the calibration curves for these analytes display direct proportionality is an indication that they dissolve well in 3-AQ/CHCA once sufficient contact time is provided for their dissolution.

The experiment for case A ($r_A < r_M$) was carried out to check whether all of the analytes lying inside a matrix circle would be transferred to the matrix layer if the process was allowed and if a sufficiently long contact time was provided. In the actual experiments, r_A and r_M were approximately 60 and 100 μm, respectively. A r_D value of 60 μm was used. In the experiment for case A, a variation in r_D did not affect the experimental result as long as it was smaller than r_M. The analyte layers containing four different amounts of Y_5R; i.e., 0.03, 0.10, 0.30, and 1.0 pmol were prepared. For each sample, we determined the concentration of Y_5R in the matrix layer using our quantification method. Because the sample is a homogeneous liquid, we can

evaluate the analyte amount simply by multiplying the amount of the liquid matrix by the analyte concentration. These results are listed in Table 4.1 together with the prepared amounts. We found that all of the Y_5R that had been in contact with 3-AQ/CHCA was completely transferred to the liquid matrix layer, as expected.

In an actual profiling or imaging process, the area occupied by an analyte can be larger than that by the matrix, i.e., $r_M < r_A$. In such a case, there is a possibility that part of the analyte lying outside of the matrix circle may somehow enter into the matrix layer. We prepared and investigated two different types of samples, denoted here as cases B and C, for a closer look at the situation.

A schematic drawing of the samples used in the experiment for case B is shown in Figure 4.1(b). In the actual experiment, we prepared analyte (Y_5R) layers with a r_A value as large as 1000 μm and with a surface molar density of 3.2 pmol/mm^2. As noted previously, the r_D value of a matrix solution drop was 60 μm. We prepared matrix layers with r_M values comparable to or larger than those of r_D by loading and drying many such drops. The r_M values of the samples prepared for the case B experiment were 60, 100, 150, and 210 μm. The experimental data are listed in Table 4.1. The measured values

of S_M are also listed in the table. By multiplying the surface molar density by S_M, the amount of the analyte in contact with the liquid matrix is obtained. This is also listed in the table. The analyte concentration in each sample was determined by our method.[48] The amount of the analyte in each sample was obtained by multiplying this by the amount of the matrix. These results are in Table 4.1. It is seen that the amount of Y_5R determined by MALDI with a liquid matrix is in good agreement with the actually prepared amount inside the matrix circle. That is, the data obtained in the experiments of cases A and B show that only Y_5R inside the matrix circle, not more and not less, is transferred into the liquid matrix layer and quantified. It is important to note that we wished to test the quantitative analyte extraction with a liquid matrix using a larger surface concentration of Y_5R than that tested in this work. One practical difficulty was that an excessively large amount of Y_5R was needed, making the experiment very costly. One can suggest reducing the cost by drawing an analyte circle with the radius smaller than 1000 μm. This method cannot be applied because most of the analyte solution volume was used simply to fill the μMatrix Spotter. That is, only a tiny fraction of it was used to draw the analyte circle.

In the experiments on cases A and B, we made sure that r_D was smaller

than that of the matrix circle (r_M) that eventually formed after the evaporation of the solvent. Suppose that r_D is larger than r_M (Figure 4.1(c)). Then, there is a chance that some of the analytes lying outside of the matrix circle, but inside the matrix solution drop circle, may be dissolved by the solvent of the matrix solution, enter into the matrix circle, contribute to the MALDI signal from the matrix layer, and hence cause positive errors in the quantified amounts. The case C experiment was carried out to check such a possibility.

As listed in Table 4.1, the r_A, r_M, and r_D values of the samples used in the case C experiments were 1000, 60, and 100 μm, respectively. The theoretical amounts of Y_5R in the samples prepared for the case C experiments were estimated based on the assumption that only those lying inside the matrix circle were transferred to the matrix layer. This result is listed in Table 4.1. The amount of Y_5R determined from three sets of data acquired by our quantification method is also listed in the table. The measured analyte amount is clearly larger than the theoretical estimation. This indicates that some of the analytes lying outside of the matrix circle, but inside of the matrix solution drop circle, move into the matrix circle in this case. However, it is unclear which of, or whether both of the two liquids, i.e., the liquid

matrix and its solvent, are responsible for the analyte movement. One thing that is clear is that r_D must be kept smaller than r_M for quantitative profiling.

Thus far, we have shown that the second step of the analyte transfer, i.e., from the sample surface to the matrix layer, occurs quantitatively in MALDI with a liquid matrix as long as the analyte dissolves well in the liquid matrix. For the quantitative profiling of an analyte located inside a solid sample, we need information about the first step, i.e., the bulk-to-surface analyte transfer process, which is not available at this time.

For a real sample, the presence of large amounts of contaminants can result in significant matrix suppression, which is an obstacle to quantitative profiling.[43,76] Further study is needed to evaluate the performance of liquid matrixes in such cases.

4.4. Conclusions

One of the advantages of using a liquid matrix in MALDI is that the samples prepared with the matrix are homogeneous. Another important advantage is the fact that the ablation temperature can easily be fixed. These two factors make it easy to acquire reproducible MALDI spectra, which, in turn, allows quantitative profiling by MALDI. A liquid matrix loaded onto a sample is expected to continue to extract analytes on the sample as long as it remains fluidic. Quantitative analyte layer-to-liquid matrix transfer of analytes in contact with the matrix layer observed in this work is compatible with the above speculation. To summarize, only those analytes, not more and not less than those in contact with a liquid matrix, are extracted by the liquid matrix. We also showed that the quantitativeness of profiling broke down when the size of the matrix solution drop initially loaded was large, i.e., larger than that of the matrix circle eventually prepared.

References

(1) Hillenkamp, F.; Peter-Katalinić, J. *MALDI MS. A practical guide to instrumentation, methods and applications.*; Wiley-VCH: Weinheim, 2007.

(2) Cole, R. B. *Electrospray and MALDI mass spectrometry. Fundamentals, instrumentation, practicalities, and biological applications*, 2nd ed.; Wiley: Hoboken, 2010.

(3) Drisewerd, K. *Chem. Rev.* **2003**, *103*, 395-425.

(4) Knochenmuss, R. *Analyst* **2006**, *131*, 966-986.

(5) Bantscheff, M.; Schirle, M.; Sweetman, G.; Rick, J.; Kuster, B. *Anal. Bioanal. Chem.* **2007**, *389*, 1017-1031.

(6) Anderson, N. L.; Anderson, N. G.; Haines, L. R.; Hardie, D. B.; Olafson, R. W.; Pearson, T. W. *J. Proteome Res* **2004**, *3*, 235-244.

(7) Parker, L.; Engel-Hall, A.; Drew, K.; Steinhardt, G; Heiseth, D. L.; Jabon, D.; McMurry, T; Angulo, D. S.; Kron. S. J. *J. Mass Spectrom.* **2008**, *43*, 518-527.

(8) Randolph, T. W.; Mitchell, B. L.; McLerran, D. F.; Lampe, P. D.; Feng, Z. *Mol. Cell. Proteomics* **2005**, *4*, 1990-1999.

(9) John, H.; Walden, M.; Schäfer, S.; Genz, S.; Forssmann, W. *Anal. Bioanal. Chem.* **2004**, *378*, 883-897.

(10) Cohen, L. H.; Gusev, A. I. *Anal. Bioanal. Chem.* **2002**, *373*, 571-586.

(11) Szájli, E.; Fehér, T.; Medzihradszky, K. F. *Mol. Cell. Proteomics* **2008**, *7*, 2410-2418.

(12) Glish, G. L.; Vachet, R. W. *Nat. Rev. Drug Discovery* **2003**, *2*, 140-150.

(13) Duncan, M. W.; Roder, H.; Hunsucker, S. W. *Brief Funct. Genomic Proteomic* **2008**, *7*, 355-370.

(14) Gerber, S. A.; Rush, J.; Stemman, O.; Kirschner, M. W.; Gygi, S.P. *Proc. Natl. Acad. Sci. USA* **2003**, *100*, 6940-6945.

(15) Oda, Y.; Huang, K.; Cross, F. R.; Cowburn, D.; Chait, B. T. *Proc. Natl. Acad. Sci. USA* **1999**, *96*, 6591-6596.

(16) Ong, S.; Blagoev, B.; Kratchmarova, I.; Kristensen, D. B.; Steen, H.; Pandey, A.; Mann, M. *Mol. Cell. Proteomics* **2002**, *1*, 376-386.

(17) Wang. S.; Kaltashov, I. A. *J. Am. Soc. Mass Spectrom.* **2012**, *23*, 1293-1297.

(18) Ong, S.; Mann, M. *Nat. Chem. Biol.* **2005**, *1*, 252-262.

(19) Kuzyk, M. A.; Smith, D.; Yang, J.; Cross, T. J.; Jackson, A. M.; Hardie, D. B.; Anderson, N. L.; Borchers, C. H. *Mol. Cell. Proteomics* **2009**, *8*, 1860-1877.

(20) Gygi, S. P.; Rist, B.; Gerber, S. A.; Turecek, F.; Gelb, M. H.; Aebersold, R. *Nat. Biotechnol.* **1999**, *17*, 994-999.

(21) Ross. R. L.;Huang, Y. N.; Marchese, J. N.; Williamson, B.; Parker, K.; Hattan, S.; Khainovski, N.; Pillai, S.; Dey, S.; Daniels, S.; Purkayastha, S.; Juhasz, P.; Martin, S.; Bartlet-Jones, M.; He, F.; Jacobson, A.; Pappin, D. J. *Mol. Cell. Proteomics* **2004**, *3*, 1154-1169.

(22) Wiese, S.; Reidegeld, K. A.; Meyer, H. E.; Warscheid, B. *Proteomics* **2007**, *7*, 340-350.

(23) Bae, Y. J.; Park, K.M.; Kim, M.S. *Anal. Chem*. **2012**, *84*, 7107-7111.

(24) Bae, Y. J.; Moon, J. H.; Kim, M. S. *J. Am. Soc. Mass Spectrom.* **2011**, *22*, 1070-1078.

(25) Kinsel, G. R.; Yao, D.; Yassin, F. H.; Marynick, D. S. *Eur. J. Mass Spectrom.* **2006**, *12*, 359-367.

(26) Bae, Y. J.; Yoon, S. H.; Moon, J. H.; Kim, M.S. *Bull. Korean Chem. Soc.* **2010**, *31*, 92-99.

(27) Moon, J. H.; Yoon, S. H.; Kim, M. S. *Bull. Korean Chem. Soc.* **2005**, *26*, 763-768.

(28) Yoon, S. H.; Moon, J. H.; Kim, M. S. *J. Am. Soc. Mass Spectrom.* **2010**, *21*, 1876-1883.

(29) Moon, J. H.; Shin, Y. S.; Bae, Y. J.; Kim, M.S. *J. Am. Soc. Mass Spectrom.* **2012**, *23*, 162-170.

(30) Bae, Y. J.; Shin, Y. S.; Moon, J. H.; Kim, M. S. *J. Am. Soc. Mass Spectrom.* **2012**, *23*, 1326-1335.

(31) Knochenmuss, R.; Stortelder, A.; Breuker, K.; Zenobi, R. *J. Mass Spectrom.* **2000**, *35*, 1237-1245.

(32) Demeure, K.; Gabelica, V.; De Pauw, E. A. *J. Am. Soc. Mass Spectrom.* **2010**, *21*, 1906-1917.

(33) Yoon, S. H.; Moon, J. H.; Kim, M. S. *J. Am. Soc. Mass Spectrom.* **2011**, *22*, 214-220.

(34) Salzer, R.; Siesler, H. W. *Infrared and Raman Spectroscopic Imaging*.; Wiley-VCH: Weinheim, 2009.

(35) Ntziachristos, V. *Annu. Rev. Biomed. Eng*. **2006**, 8, 1-33.

(36) Caprioli, R. M.; Farmer, T. B.; Gile, J. *Anal. Chem*. **1997**, *69*, 4751-4760.

(37) Cornett, D. S.; Reyzer, M. L.; Chaurand, P.; Caprioli, R. M. *Nat. Methods* **2007**, *4*, 828-833.

(38) Chughtai, K.; Heeren, R. M. A. *Chem. Rev*. **2010**, *110*, 3237-3277.

(39) Nemes, P.; Vertes, A. *Anal. Chem*. **2007**, *79*, 8098-8106.

(40) Benninghoven, A.; Rudenauer, F. G.; Werner, H. W.; *Secondary Ion Mass Spectrometry: Basic Concepts, Instrumental Aspects, Applications and Trends*.; Wiley-Interscience: Hoboken, 1987.

(41) Mahoney, C. M. *Mass Spectrom. Rev*. **2010**, *29*, 247-293.

(42) Chaurand, P.; Schwartz, S. A.; Caprioli, R. M. *Anal. Chem*. **2004**, *76*, 86A-93A.

(43) Heeren, R. M. A.; Kükrer-Kaletaş, B.; Taban, I. M.; MacAleese, L.; McDonnell, L. A. *Applied Surface Science* **2008**, *255*, 1289-1297.

(44) Lanni, E. J.; Rubakhin, S. S.; Sweedler, J. V. *Journal of Proteomics* **2012**, *75*, 5036-5051.

(45) Pirman, D. A.; Reich, R. F.; Kiss, A.; Heeren, R. M. A.; Yost, R. A. *Anal. Chem*. **2013**, *85***,** 1081-1089.

(46) Puolitaival, S. M.; Burnum, K. E.; Cornett, D. S.; Caprioli, R. M. *J. Am. Soc. Mass Spectrom*. **2008**, *19*, 882-886.

(47) Hardouin, J. *Mass Spectrom. Rev*. **2007**, *26*, 672-682.

(48) Park, K. M.; Bae, Y. J.; Ahn, S. H.; Kim, M. S. *Anal. Chem*. **2012**, *84*, 10332-10337.

(49) Ahn, S. H.; Bae, Y. J.; Moon, J. H.; Kim, M. S. *Anal. Chem*. **2013**, *85*, 8796-8801.

(50) Moon, J. H.; Yoon, S. H.; Kim, M. S. *J. Phys. Chem. B* **2009**, *113*, 2071-2076.

(51) Ahn, S. H.; Park, K. M.; Bae, Y. J.; Kim, M. S. *J. Am. Soc. Mass Spectrom*. **2013**, *24*, 868-876.

(52) Sugiura, Y.; Shimma, S.; Setou, M. *J. Mass Spectrom. Soc. Jpn*. **2006**, *54*, 45-48.

(53) Shanta, S. R.; Zhou, L. H.; Park, Y. S.; Kim, Y. H.; Kim, Y. J.; Kim, K, P. *Anal. Chem*. **2011**, *83*, 1252-1259.

(54) Bae, Y. J.; Choe, J. C.; Moon, J. H.; Kim, M. S. *J. Am. Soc. Mass Spectrom*. **2013**, *24*, 1807-1815.

(55) Aerni, H. R.; Cornett, D. S.; Caprioli, R. M. *Anal. Chem*. **2006**, *78*, 827-834.

(56) Shrestha, B.; Patt, J. M.; Vertes, A. *Anal. Chem*. **2011**, *83*, 2947-2955.

(57) Jun, J. H.; Song, Z.; Liu, Z.; Nikolau, B. J.; Yeung, E. S.; Lee, Y. J.

Anal. Chem. **2010**, *82*, 3255-3265.

(58) Lanni, E. J.; Rubakhin, S. S.; Sweedler, J. V. *J. Proteome Res.* **2012**, *75*, 5036-5051.

(59) Bantscheff, M.; Lemeer, S.; Savitski, M. M.; Kuster, B. *Anal. Bioanal. Chem.* **2012**, *404*, 939-965.

(60) Brown, R. S.; Lennon, J. J. *Anal. Chem.* **1995**, *67*, 3990-3999.

(61) Park, K. M.; Moon, J. H.; Kim, K. P.; Lee, S. H.; Kim, M. S. *Anal. Chem.* **2014**, *86*, 5131-5135.

(62) Norris, J. L.; Caprioli, R. M. *Chem. Rev.* **2013**, *113*, 2309-2342.

(63) Quiason, C. M.; Shahidi-Latham, S. K. *J. Am. Soc. Mass Spectrom.* **2015**, *26*, 967-973.

(64) Ahn, S. H.; Park, K. M.; Moon, J. H.; Lee, S. H.; Kim, M. S. *J. Mass Spectrom.* **2015**, *29*, 745-752.

(65) Baluya, D. L.; Garrett, T. J.; Yost, R. A. *Anal. Chem.* **2007**, *79*, 6862-6867.

(66) Bae, Y. J.; Park, K. M.; Ahn, S. H.; Moon, J. H.; Kim, M. S. *J. Am. Soc. Mass Spectrom.* **2014**, *25*, 1502-1505.

(67) Schwartz, S. A.; Reyzer, M. L.; Caprioli, R. M. *J. Mass Spectrom.* **2003**, *38*, 699-708.

(68) Schulz, S.; Gerhardt, D.; Meyer, B.; Seegel, M.; Schubach, B.; Hopf, C.; Matheis, K. *Anal. Bioanal. Chem.* **2013**, *405*, 9467-9476.

(69) Kaletaş, B. K.; van der Wiel, I. M.; Stauber, J.; Dekker, L. J.; Güzel, C.; Kros, J. M.; Luider, T. M.; Heeren, R. M. A. *Proteomics* **2009**, *9*, 2622-2633.

(70) Gusev, A. I.; Wilkinson, W. R.; Proctor, A.; Hercules, D. M. *Anal. Chem*. **1995**, *67*, 1034-1041.

(71) Park, K. M.; Moon, J. H.; Kim, J. H.; Song, U. T.; Lee, S. H.; Kim, M. S. *Rapid Commun. Mass Spectrom.* **2016**, *30*, 386-392.

(72) Armstong, D. W.; Zhang, L.; He, L.; Gross, M. L. *Anal. Chem*. **2001**, *73*, 3679-3686.

(73) Li, Y. L.; Gross, M. L. *J. Am. Soc. Mass Spectrom*. **2004,** *15*, 1833-1837.

(74) Meriaux, C.; Franck, J.; Wisztorski, M.; Salzet, M.; Fournier, I. *J. Proteomics* **2010**, *73*, 1204-1218.

(75) Moon, J. H.; Park, K. M.; Ahn, S. H.; Lee, S. H.; Kim, M. S. *J. Am. Soc. Mass Spectrom*. **2015**, *10*, 1657-1664.

(76) Groseclose, M. R.; Castellino, S. *Anal. Chem*. **2013**, *85*, 10099-10106.

Publication List

1. “Host-Guest Chemistry in the Gas Phase: Selected Fragmentations of CB[6]- Peptide Complexes at Lysine Residues and Its Utility to Probe the Structures of Small Proteins” S. W. Heo, T. S, Choi, K. M, Park, Y. H, Ko, S. B, Kim, K. M, Kim, and H. I. Kim *Anal. Chem*. (2011), 83, 7916-7923

2. “Reproducibility of Temperature-Selected Mass Spectra in Matrix-Assisted Laser Desorption Ionization of Peptides” Y. J. Bae, K. M. Park, and M. S. Kim *Anal.Chem.* (2012), 84, 7107-7111

3. “A Simple Method for Quantification of Peptides and Proteins by Matrix-Assisted Laser Desorption Ionization Mass Spectrometry” K. M. Park, Y. J. Bae, S. H. Ahn, and M. S. Kim *Anal.Chem.* (2012), 84, 10332-10337

4. “Quantitative reproducibility of mass spectra in matrix-assisted laser desorption ionization and unraveling of the mechanism for gas-phase peptide ion formation” S.H. Ahn, K. M. Park, Y. J. Bae, and M. S. Kim *J. Mass Spectrom.* (2013), 48, 299-305

5. “Efficiency of Gas-Phase Ion Formation in Matrix-Assisted Laser Desorption Ionization with 2,5-Dihydroxybenzoic Acid as Matrix” K. M. Park, S.H. Ahn, Y. J. Bae, and M. S. Kim *Bull. Korean Chem Soc.* (2013), 34, 907-911

6. “Efficient Methods to Generate Reproducible Mass Spectra in Matrix-Assisted Laser Desorption Ionization of Peptides” S.H. Ahn, K. M. Park, Y. J. Bae, and M. S. Kim *J. Am. Soc. Mass. Spectrom.* (2013), 24, 868-876

7. "Efficiency of Gas-Phase Ion Formation in Matrix-Assisted Laser Desorption Ionization with 2,5-Dihydroxybenzoic Acid as Matrix", K. M. Park, S. H. Ahn, Y. J. Bae, and M. S. Kim, *Bull. Korean Chem. Soc*. 34(3), 907-911 (2013)
8. “Thermal determination of the abundances of c and z type fragment ions generated by in-source decay of peptide ions in matrix-assisted laser desorption ionization” K. M. Park, Y. J. Bae, J. H. Moon, and M. S. Kim *Int. J. Mass Spectrom* (2013), 352, 70-76

9. “Relative Quantification in Imaging of a Peptide on Mouse Brain Tissue by Matrix-Assisted Laser Desorption Ionization” K. M. Park, J. H. Moon, K. P. Kim, S. H. Lee, and M. S. Kim *Anal. Chem.* (2014), 86, 5131-5135

10. “Spectral Reproducibility and Quantification of Peptides in MALDI of Samples Prepared by Micro-Spotting” Y. J. Bae, K. M. Park, S. H. Ahn, J. H. Moon, and M. S. Kim *J. Am. Soc. Mass Spectrom* (2014), 25, 1502-1505

11. “Acquisition of the depth profilies and reproducible mass spectra in matrix-assisted laser desorption/ionization of inhomogeneous samples” S.

H. Ahn, K. M. Park, J. H. Moon, S. H. Lee, and M. S. Kim *Rapid commun. Mass Spectrom* (2015), 29, 745-752

12. “Investigations of some liquid matrixes for quantification by MALDI” J. H. Moon, K. M. Park, S. H. Ahn, S. H. Lee, and M. S. Kim *J. Am. Soc. Mass Spectrom* (2015), 10, 1657-1664

13. "Preparation of homogeneous solid samples for reproducible and quantitative MALDI", S. H. Ahn, K. M. Park, J. H. Moon, S. H. Lee and M. S. Kim, *Bull. Korean Chem. Soc.* 37(4), 458-462 (2016)

14. "Use of Commercial MALDI-TOFs for Analyte Quantification by a Newly Invented Method", K. M. Park, S. H. Yoon, J. H. Moon, S. H. Lee and M. S. Kim, *Bull. Korean Chem. Soc.* 37(6), 882-885 (2016)

15. “Discovery of a solvent effect preventing quantitative profiling by matrix assisted laser desorption ionization and its treatment” K. M. Park J. H. Moon, J. H. Kim, U. T. Song, S. H. Lee, and M. S. Kim *Rapid commun. Mass Spectrom* (2016), 30, 386-392